Advanced Control of a fed-batch reaction system to increase the yield in the polyhydroxyalkanoates production process.

CESAR AUGUSTO GARCÍA ECHEVERRY
Chem.Eng.

Thesis work presented as partial requirement to qualify for the Master degree in Chemical Engineering.

ADVISORS: M.Sc., Dr. Ing. Silvia Ochoa Cáceres
M.Sc Alejandro Acosta Cárdenas

Master Program in Chemical Engineering
Universidad de Antioquia
Medellín-Colombia
2016

ACKNOWLEDGEMENTS

I would firstly like to thank God for giving me strength and discernment.

Very special thanks and to convey my sincere gratitude to Professor Dr. Silvia Ochoa for all her advice, and encouragement throughout the studies, research and personal life, for all the support and trust, along with my co-supervisor Professor M.Sc Alejandro Acosta for initiating the project and always being on hand to provide helpful comments.

Very special thanks to Professor Dr Rosario Caicedo, for her trust, support and advice throughout the young researcher project and my studies, along with Professor M.Sc Gezira de Avila for giving me advice and encouragement to continue.

I am very grateful to all those who have helped me and taken an interest in the project. Special thanks go to SIDCOP and BIOTRANSFORMACIÓN research groups for the knowledge and learning, to my co-workers and professors in general.

Many thanks to my family, for the support and advice, specially my uncles Lucia Echeverry and Julio Echeverry for so kindly providing logistic support for the trip to Medellin.

Special thanks to Wilman Alcaraz for helpful discussions, and support during the development of this work.

Financial support from the Universidad de Antioquia and Colciencias through the project CIEMB-107-14 and CIEMB-125-2015 (065-2015 COLCIENCIAS) is gratefully acknowledged.

Last, but certainly not least, I am grateful to Kathleen Navarro, my occasional chef and Brandy, for being my workmate when I had to work until late, and my friends in general.

TABLE OF CONTENTS

LIST OF FIGURES

LIST OF TABLES

ABSTRACT

Plastics are one of the main products of the petrochemical industry, due to its wide variety of physical and chemical properties. However, the intensive use of plastics has created an important environmental problem, and therefore, many alternatives are currently explored for reducing it. The Polyhydroxyalkanoates (PHAs) are polymers from biological origins, which are an environmentally friendly option for replacing the use of petroleum based plastic materials in a wide number of applications [1], [2]. Currently, big companies in China, United States, Brazil and Canada are carrying out the production of PHAs at industrial level. However, in order to replace or at least to compete against the petroleum –based plastic materials, it is still needed to assure the technical and economic feasibility of the process. For this reason, it is important to develop strategies towards increasing the yield of the process. For this, advanced model-based control strategies must be applied instead of the classical control strategies, which have shown to be inefficient in many bioprocess applications [3], [4], [5] and [6]. Since 2012, the biotransformation research group at Universidad de Antioquia has conducted research projects towards finding a technical and economical feasible alternative for producing PHAs using Colombian agricultural wastes. Preliminary results obtained at bioreactor scale have shown to be promising assuring the technical feasibility of the production process. However, in order to increase the productivity of the process for assuring its economic feasibility, optimization and control tools are proposed to be used in this master thesis. In this work, the optimizing control of the PHAs fed-batch process is carried out by formulating and solving a dynamic optimization problem for maximizing the process productivity. The optimization problem is subject to constraints on the feed flow rates, the final volume and the maximum concentrations reached on the substrate and nitrogen source, in order to avoid inhibition. Furthermore, the number average molecular weight distribution (Mn) is predicted using state estimation strategy and is used as constraint in order to fulfill desired end-product specifications. By solving the problem stated, it was possible to find the optimal values for the substrate and the nitrogen-source feed concentrations, as well as their optimal feeding profiles that maximize the process productivity. Solution of the dynamic optimization problem was carried out by the

control vector parameterization approach. Different kinds of parameterization for the control vector were tested in order to compare their advantages and disadvantages. Results of the dynamic optimization problem have shown that sinusoidal type control profiles lead to higher productivity values (i.e. in comparison to step-type or constant feeding policies), while fulfilling the constraints, being remarkable that the number average molecular weight was kept around $4.05x10^5$ g/mol and the productivity of the final amount of polymer over 138.44 g or 0.62 g/Lh for a 32 h fermentation and a final volume of 7 L. Finally, it was shown that the optimizing control strategy coupled to the prediction of Mn is an interesting and applicable alternative that could help to improve the PHAs productivity at industrial scale. Further work will be directed towards applying the mentioned strategy experimentally at pilot plant scale.

Keywords: Polyhydroxyalkanoates, dynamic optimization, Soft-Sensors, Advanced control.

1. STATE OF THE ART

Since 1970, the strain *Ralstonia eutropha* was recognized as a strain with a greater capacity to produce Polyhydroxyalkanoates (PHAs). From that moment, numerous works have been carried out in order to get a deep understanding of this bacterium. The development of molecular biology in recent decades, also allowed obtaining new tools for biological research that helped in deciphering the genetic information and the biosynthesis of PHAs. In the late 1980s, the genes encoding enzymes involved in the biosynthesis of PHAs were inserted into *Ralstonia eutropha* strains and *E. coli*. In the mid-90s, two *R. eutropha* studies allowed to establish the three most important enzymes in the metabolic pathway of this organism for biosynthesis of the biopolymer. In addition, it was identified that the PHA synthase was intracellular allowing polymerization. The success of genetic modification of microorganisms to promote the production of PHAs has led to the generation of transgenic plants that accumulate the polymer and have established the potential to expand the production at industrial level [7], [8].

At the industry level, first industrial production of poly-3-hydroxybutyrate-co-3-hydroxyvalerate (P (HB-co-HV)) was started in 1982 [9]. On that year, the British company Imperial Chemical Industries Ltd (ICI) started the production of a biodegradable thermoplastic polyester called Biopol^{TM}, which was employed in the preparation of films and fibers [10]. The technology used involved a fermentation process on a large scale; with the intracellular accumulation of polymer equal to 90% of the cell weight of bacteria *Alcaligenes eutrophus*, later renamed as *Ralstonia eutropha*.

In the 90s, the bacterial fermentation of PHAs was commercially available by Zeneca and then by Monsanto under the trade Biopol^{TM} brand, however, the costs of production of PHBV were too high (about 6.60 USD / kg) due the fermentation and separation technology available at that time and failed to be cost competitive when compared to conventional plastics [9]. Meanwhile, in the same period Metabolix, Inc. developed a PHAs fermentation technology at lower cost (below $ 2.20 / kg), which allowed the

company to reach a commercial-scale production of PHAs [10]. All this industrial efforts have opened the market of new biomaterials in the world.

There are currently over 19 PHAs production companies worldwide, 6 in China, 3 in United States and 6 in Canada, there exist potential for new companies; 4 in Europe, 2 in Japan and 1 in Brazil. In Brazil, PHB Industrial SA, uses sugar cane to manufacture PHB with Biocycle^{TM} registered brand. This company started since 1992 and it is a partnership between the sugar producer Irmãos Biagi and the alcohol producer Balbo Group. By 2010, the company produced 4,000 tons per year and plans to increase its production capacity to 14,000 tons per year [10]. Although it has been seen that there is already available technologies for PHAs production at industrial level, the production of these biopolymers does not reach the expected volumes due to high operating costs. According to [11], [12], in the United States, the production costs of PHAs are five times higher than the production costs of petrochemical-based thermoplastics. The review presented in [13], discusses several research works dedicated to the production of PHAs from sustainable raw materials of low cost, such as molasses, whey, and wastewater from oil producing plants, among other works. The works presented in [14], [3], [15] and [16] reported the use of whey as raw material. Reports shown in references [17], [18], [19] and [20] studied the production of PHAs using nutrients from the wastewater (from different types of industries, including municipal wastewater). Although most works reported that it is technically feasible to produce PHAs from the low-cost raw materials mentioned, it is important to note that the raw material resulting in the best performance (in terms of higher PHAs concentration) was obtained by using sugar cane molasses [21]. However, from an industrial point of view, in Colombia, using sugarcane molasses as the sole substrate of the process would not be considered profitable because this is not a low-cost feedstock in the country.

Different modes of operation (batch, fed batch and continuous) have been used for producing PHAs. The Continuous operation has the advantage of achieving high yields and productivity but have a high risk of contamination. Batch production is a more conventional process, but several works have reported that higher productivities can be

achieved in Fed Batch operation [22]. The different production strategies depend on various factors such as the carbon source, the culture (pure or mixed), type of bioreactor (bubble columns or stirred tank) and operation mode (Batch, Fed Batch or Continuous). Productivities reported in [23] using sugar cane molasses as carbon source in batch cultures by *P. aeruginosa* are close to 0.1 g/Lh. In reference [24], reported productivities are around 0.45 g / Lh by *B. megaterium* using molasses. On the other hand, [24] reported productivities around 1.27 g / Lh for the same raw material, but using a Fed-batch reactor. The advantage of operating in fed-batch mode is that the carbon source and other nutrients are provided at a different rate during the process, depending on the culture stage. Therefore, some stress conditions can be induced which has shown to increase the accumulation of biopolymer.

In Table 1, a summary of the most relevant works in the modeling of the PHAs process is presented.

Table 1. Models Proposed in the literature for PHAs production.

State Variables	Type of Model	Microorganism	Reference
Biomass, Substrates and Product Concentration	Structured and metabolic model	Animal cells	[15]
Biomass, Fructose, Nitrogen and PHB concentration	Unstructured Model	*Alcaligenes eutrophus*	[3]
Biomass, Intracelular PHB, Substrate and acetate Concentration	Unstructured Model	*Paracoccus Pantotrophus*	[16]
Biomass, polymer, carbon and nitrogen sources And oxygen.	Unstructured Model	*Azohydromonas Lata*	[17]
Biomass, Nitrogen, Fructose and PHB concentration	Unstructured Model	*Wautersia eutropha*	[18]

On the other hand, it is important to notice that in recent years much effort has been done from the academia in order to achieve higher productivity in bioprocesses, including the biopolymers production. Many of these works have used tools from the Process Systems Engineering (PSE) for addressing the modeling, optimization and control of the process. Many advanced control strategies have been already applied for controlling bioprocesses. For example, in [3], the authors implemented a model predictive controller (MPC) accompanied with a metabolic reaction model controller for controlling ethanol and n-pentanol concentrations and the mole fraction of monomer units in the production of poly(β-hydroxybutyrate-co-β-hydroxyvalerate), P(HB-co-HV), a biodegradable co-polyester. Ethanol and n-pentanol concentrations were well controlled by the MPC, compared with Proportional-Integral (PI) controller and feedforward/feedback controller. As a result, P(HB-co-HV) production was maximized with a given value of mole fraction of 3HV units at the end of cultivation. In another application, in [25] the authors deal with a hybrid adaptive feeding control strategy for fed-batch cultivation of high cell density *Escherichia coli* (*E. coli)*. The control strategy was designed in order to maintaining the growth of the cells in optimal critical value despite disturbances and modeling uncertainties. For this purpose first an optimal controller was suggested by the authors and it was made such that fosters the growth rate to the optimal critical value and then a sliding mode controller (SMC) was applied, which powerfully strengthens the optimal controller against disturbances and uncertainties. The combined controller is capable of achieving the maximum amount of biomass and recombinant protein production despite a large number of uncertainties and disturbances. In [26], [27] and [28] the authors applied second-order sliding observer based on biomass concentration measurement, multiple kinetic rates observer and on-line measurements, in order to get a practical stabilizer, by combining the observer with an input–output linearizing controller and provides a smooth estimate that converges in finite time to the time-varying parameter. On the other hand, in [29] and [30], the authors propose a robust nonlinear control in order to decrease the trajectory disturbances. The proposed controller is proven to guarantee the uniform ultimate boundedness of the closed-loop system by the Lyapunov theory.

For implementing successfully advanced control strategies, it is necessary to monitor the main process variables, and particularly in biopolymer´s production, it is highly desirable to monitor end-product specifications on-line. However, it is well known that difficulties arise on monitoring bioprocesses. Different strategies have been applied to overcome such difficulties, which include the development of Kalman filters and state observers. According to [4] a system is said to be observable if we can estimate the state variables from the available measurements, but first it is necessary determine the observability of the system. In [4] the author propose many ways to build an observer, depending if the system is linear or non-linear and for each one there is an observer, like Luenberger Observer, PI observer, and the different versions of the Kalman Filter. In [31] and [32] the authors deal with some classical state estimation techniques for bioprocess applications, the extended Kalman filter and the asymptotic observer, as well as a more recent technique based on particle filtering. In this application context, all these techniques are based on a continuous-time nonlinear prediction model and discrete-time measurements. A hybrid asymptotic particle filter was proposed, which combines the advantages of both techniques (robustness to model uncertainties and a rigorous consideration of the process and measurement noises).

On the other hand, recent published works in the literature apply modelling and optimization tools for improving the productivity specifically in the PHAs process [33], [8], [34], [35], [36]. The work presented in [14], deserves special attention. In that work, the application of Multi-Objective Optimization (MOO) was carried out to find suitable feeding profiles in order to maximize the productivity of the PHAs process in a 9-liter bioreactor. The authors proposed the multi-objective for finding a compromise between productivity maximization and minimization of the frequency of gradual changes in the actuator. Many authors have studied the fed- batch fermentations (fed-batch) to improve production yields of PHAs. Improving the production of PHAs is generally achieved through the establishment of special feeding conditions. These techniques have been developed on an experimental basis and procedures of trial and error. The results have shown a considerable increase in the productivity of PHB with respect to previous works. However, the trial and error procedures can easily result in sub-and over-feeding of the

substrate, which can lead to cell starvation, cell inhibition, and the formation of undesirable products. On the other hand, some authors have developed multiple fed-batch experiments to increase the productivity of PHAs. They have focused on obtaining a phase of high cell density, followed by a high production of PHAs by a non-growth-associated mechanism. For example, some authors recommend that for an efficient production of PHAs by *Alcaligenes eutrophus*, the concentration of the carbon source must be maintained at an optimum value [3]. In [3] dynamic optimization of PHAs production process in fed-batch operation using fructose as a carbon source in a bioreactor of 10 liters is presented. The authors of that study concluded that dynamic optimization is an excellent tool to predict the optimum operating conditions that achieve maximum productivity of PHB, greatly reducing the time and cost of the process. Indeed, this is one of the strategies to be used in the development of this project, where PSE tools (modeling, control, optimization, etc.) will be used to improve the technical and economic feasibility in the PHAs production process using low cost substrate (i.e. wastes from the alcohol industry).

As it can be seen in Table 1, it is possible to find in the literature [37], [38], [39] and [40] that the unstructured models are well used to describe, in the simplest way, what is happening with the state variables. However, in [5] and [6] the authors proposed a combined kinetic/polymerization model in order to determine Mn and Mw.

According to [19], the development of an effective methodology for optimizing of the polyhydroxyalkanoates (PHAs) fermentation with *Ralstonia eutropha* requires online measurement of some state variables. In that work, biomass viability information was obtained by measuring on-line the capacitance. Furthermore, oxygen uptake rate, specific oxygen uptake rate and specific growth rate were measured in real-time and compared with the capacitance value. In addition, a fed-batch control strategy based on the on-line capacitance measurement was proposed and showed to improve the PHAs production by 22%. This mentioned work pointed out the need of correlating important state variables with on-line measurements in order to increase the productivity.

In the present project, it is proposed to develop soft-sensors that will be useful for applying an advanced control strategy in the real process. Soft-sensors are software-based monitoring systems. In real-time they estimate those process variables, which are difficult to measure on-line or whose measurement by analytical procedures is tedious, expensive and time-consuming. In [20], the Genetic Programming (GP), an artificial intelligence based data-driven modeling formalism, is introduced for the development of soft-sensors for biochemical processes. The novelty of the GP is that for a given input–output data, it searches and optimizes both the structure and parameters of an appropriate linear/nonlinear model. In the mentioned reference, GP-based soft-sensors were developed for two bioprocesses, the extracellular production of lipase enzyme (where the soft-sensor predicted the time-dependent lipase activity) and the bacterial production of P (HB-co-HV) copolymer (where the amount of accumulated biopolymer was predicted). As conclusion, it was shown that the GP-based soft-sensor predictions where much better than those obtained by the Neural network, but according to [41], artificial neuronal network (ANN) based soft-sensor are useful for real case control applications with a fast computational time and control output response.

In [42] the authors proposed an analytical and experimental analysis of the MWD of Poly((R)-3-hidroxy-butirate) using *Alcaligenes Latus*, in [38] the authors deal with a combined metabolic/polymerization kinetic model in order to predict the molecular weight distribution. This is very important because the molecular weight is important for establishing the final industrial application of the polymer. It determines in an important degree, the physical, chemical, mechanical and rheological characteristics of the polymer. When the weight average molecular weight (Mw) is lower than $4x10^5$ Da, the polymer cannot be used for thermoplastic applications. Additionally, typical values of the number average molecular weight (Mn) of PHB are in the range from $8x10^4$ to $1x10^6$ Da [38].

The molecular weight distribution of biopolymers is affected by many variables, including the host microorganism, the substrate type and concentration, the nutritional (e.g. nitrogen source and oxygen concentration), the operating conditions (e.g. pH and

temperature), the feeding policy (in fed-batch and continuous processes), as well as the downstream polymer separation and processing.

In order to find smooth and continuous feeding profiles (for the substrate, and the nitrogen-source) suitable for bioprocess applications operating in fed-batch mode, the work presented in [43] proposed to parameterize the control vector by using sinusoidal functions. Typical works in bioprocess applications as well as in specifically the PHAs process, uses constant, pulse-type and/or piecewise constant feeding policies. In this work, sinusoidal parameterization is compared against a constant input flow and a piecewise constant control policies.

In summary, this work addresses the advanced control problem for a fed-batch process for Polyhydroxyalkanoates production using the optimizing control strategy. Solution of the optimizing control problem is solved by formulating and solving a Dynamic Optimization problem in order to maximize the process productivity. The optimization problem is subject to constraints on the feed flow rates, the final volume and the maximum concentrations allowable to be reached on the substrate and nitrogen-source, in order to avoid inhibition. For solving the Dynamic optimization problem, different parameterization strategies of the control vector were used in order to compare their effect on the dynamic behavior of the biological variables, and therefore, on the process productivity. Furthermore, it is proposed to couple the optimizing control strategy to a neural network soft sensor developed for predicting Mn, Mw and/or the rate of polydispersity (PDI).

2. THEORETICAL FRAMEWORK

In this section, the more important aspects of the theoretical framework needed for the development of this master thesis are presented. First, the generalities about the polyhydroxyalkanoates are given. Second, the current tendency for PHA's production. Is presented, in section 2.3, a brief mention about State Estimation and dynamic optimization is carried out. Section 2.3 presents an overview for dynamic optimization applications and how it helps to get a better performance and fermentation process.

2.1 Polyhydroxyalkanoates (PHAs) Generalities

PHAs are natural polymers produced by bacteria, which can accumulate around 90 % of the dry cell weight [21]. Such polymers have attracted the attention of the scientific community due to its high biodegradability, to the physical and mechanical properties comparable to those of petroleum-based plastics and for being produced from renewable resources [22]. PHAs are a family of polyesters with optically active organic monomer units (R) - 3HA. 3 - hydroxyalkanoates acids are all in the R configuration due to the stereo specificity of the enzyme polymer, PHA synthase [23]. Concerning PHAs, it can be highlighted the thermoplastic character and / or elastomer of these materials.

Different types of PHA's can be obtained depending on the strain and the substrates used for its production. Table 2 shows the most common bacteria used at both, industrial and lab levels for PHA's production and the commonly reported values for the average molecular weight and the polydispersity of produced polymer when such bacteria are used.

Table 2 Molecular Weight for PHA's reported for different strains [44].

Polymer	Molecular Weight (g/mol)	Polydispersity Index
P3HB from *R. eutropha*	939000-1400000	1.9-2.25
PHA from *P. oleovorans*	178000-330000	1.8-2.4
PHAfrom *P. putidas*	56000-112000	1.6-2.3

As mentioned, PHAs are microbial polyesters produced by a variety of microorganisms, under conditions of nutrient limitation or excess of carbon source. PHA's exhibit significant advantages over conventional polymeric materials, as they are produced from renewable sources; they are 100% non-toxic and biodegradable. The poly (3 - hydroxybutyrate) or PHB is the most important member of the PHAs, which was the first PHA discovered and remains the most studied. It is a biopolymer with a wide range of applications since their mechanical properties are similar to conventional commercial polymers such as polypropylene. Despite the potential of PHAs, their introduction into the world market is currently limited due to a number of economic considerations [1], [7] and [45]. However, many efforts in the recent years have been done in order to speed up the development of profitable processes for PHAs production. An important point in order to improve the process is to understand the effect of the oxygen, carbon and nitrogen sources on the metabolic behavior of the bacteria responsible for the production, For example, Figure 1 shows the metabolic pathway for synthetizing PHB by *Alcaligenes* species. From this, it is possible to observe the effect of carbon, nitrogen and oxygen source in the production of biomass and polymer, besides, the direct relation between the production of CO_2 and the obtained biomass. The Etner-Doudoroff pathway explains the required electron transfer in order to obtain the biomass and polymer under stress conditions such as excess of carbon source and limitation of nitrogen and/or oxygen source.

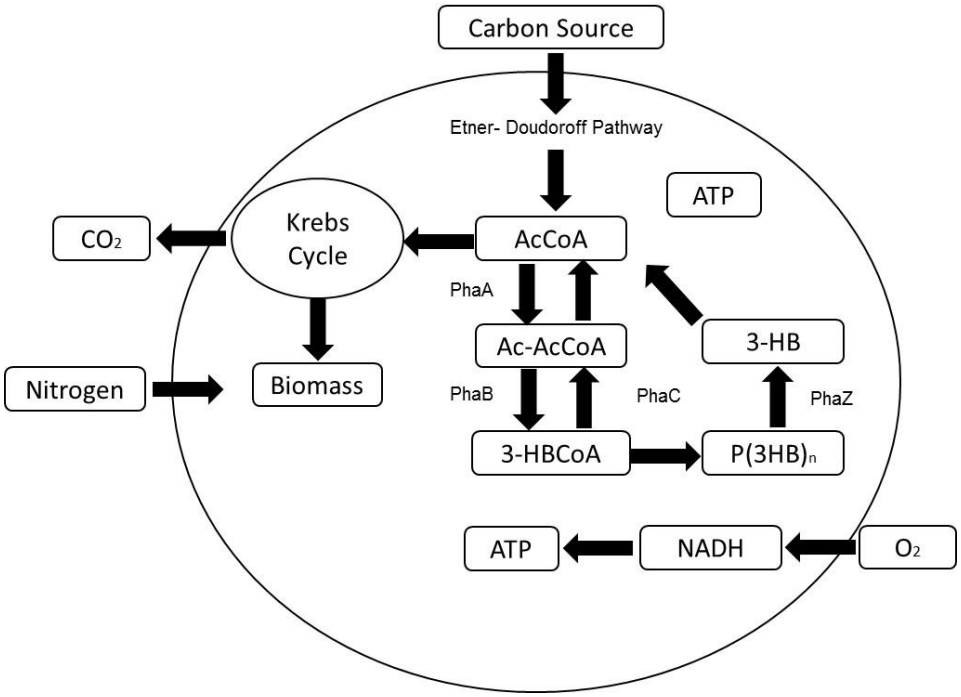

Figure 1 Metabolic pathway for the intracellular synthesis and degradation of PHB in *Alcaligenes* species [38].

The molecular structure of PHB is shown in Figure 2. It is possible to observe the presence of the carboxylic acid ester group in the main chain.

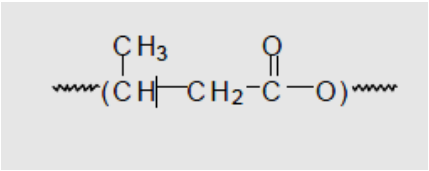

Figure 2 Chemical structure of Polyhydroxybutyrate (PHB) [24].

The average molecular weight and the polydispersity index of a polymer are important parameters that characterize the physical and mechanical properties of a polymer. There have been several reports concerning the effects of cultivation conditions, such as carbon sources, temperature, pH, and trace elements, on the molecular weight and polydispersity of bacterial polyesters. However, the mechanism for controlling the

molecular weight of PHA in vivo has not been clarified yet. Some Scientific works reported in [33] have studied the kinetics of the in vivo synthesis and degradation of P(3HB) in *R. eutropha*, and have proposed a kinetic model involving chain propagation and chain transfer reactions on the active site of PHA synthase. Although PHA synthase has been identified as a key enzyme in PHA biosynthesis, only few studies [46] and [47] have been focused on the relation between the synthase activity and the molecular weight properties of the intracellular PHA. In [47] and [48], the authors deal with the importance in the control of the final molecular weight of P(3-HB) in a fermentation process. This is due to the challenge of achieving appropriate mechanical performance characteristics for industrial applications. By this reason, the authors keeps Mn and Mw in a desired value applying feeding control strategies in order to achieve the final goal. This is varying the carbon and nitrogen source concentration using different carbon sources.

The advantages of the used strategies by the authors is that are tools easy to implement and with a good approximation of the macroscopic behavior in the fermentation process. The disadvantage is that in many cases with the macroscopic approximation is not possible get the enough information of the real kinetic and microscopic process and the deviations could be very important for the control implementation.

2.2 PHAs production

There are mainly two predominant methods used to produce PHBs depending on the microorganisms used. The most frequently applied method is a fermentation process consisting on two stages: i) a stage for cell growth under favorable conditions to provide high cell density, and ii) a stage for PHB production at unbalanced growth conditions by using limiting nutritional conditions (i.e. nitrogen, oxygen or phosphate sources limitation) to trigger the synthesis and accumulation of PHB. The second method is a process that occurs in a single-stage, in which PHB is accumulated in association with growth [34].

There exist many companies in the business of production of PHBs; The British Imperial Chemical Industries Ltd (ICI) with BiopolYMER [9]. Metabolix, Inc. developed a fermentation technology [10], which gave greater openness to new biomaterials market in the world, PHB Industrial SA, with Biocycle registered brand.

In Table 3 a complete list of worldwide PHA producing and researching companies is presented. It shows the different efforts in order to get a high productivity of many types of PHA including their applications.

Table 3 Worldwide PHA: Production and applications [49]

Company	Types of PHA	Production scale (t/a)	Period	Applications
ICI, UK	PHBV	300	1980s to 1990s	Packaging
Chemie Linz, Austria	PHB	20–100	1980s	Packaging & drug delivery
btF, Austria	PHB	20–100	1990s	Packaging & drug delivery
Biomers, Germany	PHB	Unknown	1990s to present	Packaging & drug delivery
BASF, Germany	PHB, PHBV	Pilot scale	1980s to 2005	Blending with Ecoflex
Metabolix, USA	Several PHA	Unknown	1980s to present	Packaging
Tepha, USA	Several PHA	PHA medical implants	1990s to present	Medical bio-implants
ADM, USA (with Metabolix)	Several PHA	50 000	2005 to present	Raw materials
P&G, USA	Several PHA	Contract manufacture	1980s to 2005	Packaging
Monsanto, USA	PHB, PHBV	Plant PHA production	1990s	Raw materials
Meredian, USA	Several PHA	10 000	2007 to present	Raw materials
Kaneka, Japan (with P&G)	Several PHA	Unknown	1990s to present	Packaging
Mitsubishi, Japan	PHB	10	1990s	Packaging
Biocycles, Brazil	PHB	100	1990s to present	Raw materials
Bio-On, Italy	PHA (unclear)	10 000	2008 to present	Raw materials
Zhejiang Tian An, China	PHBV	2000	1990s to present	Raw materials
Jiangmen Biotech Ctr, China	PHBHHx	Unknown	1990s	Raw materials
Yikeman, Shandong, China	PHA (unclear)	3000	2008 to present	Raw materials
Tianjin Northern Food, China	PHB	Pilot scale	1990s	Raw materials
Shantou Lianyi Biotech, China	Several PHA	Pilot scale	1990s to 2005	Packaging and medical
Jiang Su Nan Tian, China	PHB	Pilot scale	1990s to present	Raw materials
Shenzhen O'Bioer, China	Several PHA	Unknown	2004 to present	Unclear
Tianjin Green Bio-Science (+DSM)	P3HB4HB	10 000	2004 to present	Raw materials & packaging
Shandong Lukang, China	Several PHA	Pilot scale	2005 to present	Raw materials & medica

The different types of polymer are obtained due the type of strain, carbon source and feeding strategy. In Table 4 is presented the most common strains for industrial applications, including the amount and the type of polymer.

The standard fermentation conditions for the strains are; pH 7, 30°C, D.O 20-40% and time fermentation around 24 and 48 hours, depending the polymer accumulation and the feeding strategy, that is, the final manipulated variable in the control strategy.

Table 4 Strain type and industrial bacterial strains commonly used for pilot and large-scale production of PHA [49].

Strain	PHA Type	Carbon Source	Final dry cell weight (DCW) (g/L)	Final PHA (%DCW)
Ralstonia Eutropha	PHB	Glucose	>200	>80%
Ralstonia Eutropha	PHBV	Glucose + propionate	>160	>75%
Ralstonia Eutropha	P3HB4HB	Glucose + 1,4-Butanediol	>100	>75%
Ralstonia Eutropha	PHBHHx (1)	Fatty Acids	>100	>80%
Alcaligenes Latus	PHB	Glucose or Sucrose	>60	>75%
Escherichia Coli	PHB	Glucose	>150	>80%
Aeromonas hydrophila	PHBHHx (1)	Lauric Acid	<50	<50%
Pseudomonas putida	mcl PHA	Fatty Acids	~45	>60%
P. Oleovorans	mcl PHA	Fatty Acids	~45	>60%
Bacilus spp.	PHB	Sucrose	>90	>50%

2.3 State Estimation and Dynamic Optimization

The optimizing control strategy implemented in this work includes the development of an observer based soft-sensor and the solution of a dynamic optimization problem. Therefore, the theoretical framework on these two topics is briefly discussed.

2.3.1 Observers

According to [50], observers are systems whose task is state estimation. The inputs of the observer are the inputs of and the outputs of the given system. Furthermore, it is always important to estimate those states prior to developing state feedback laws for control. A recent work by [51], presents a classification of recent observers applied to chemical process systems. Such classification is shown in Table 5, where the main differences are in the linearity/nonlinearity and noise of the system.

Table 5 Recent observers categorized under different classes applied to chemical process systems. [51]**.**

Class					
Luenberger-based observers	**Finite-dimensional system observers**	**Bayesian estimators**	**Disturbance and fault detection observers**	**Artificial intelligence-based observers**	**Hybrid observers**
Specific observer					
1. Extended Luenberger observer (ELO)	1. Reduced-order observer	1. Particle filter (PF)	1. Disturbance observer (DOB)	1. Fuzzy Kalman filter	1. Extended Luenberger-asymptotic observer
2. Sliding mode observer (SMO)	2. Low-order observer	2. Extended Kalman filter (EKF)	2. Modified disturbance observer (MDOB)	2. Augmented fuzzy Kalman filter	2. Proportional-integral observer
3. Adaptive state observer (ASO)	3. High gain observer	3. Unscented Kalman filter (UKF)	3. Fractional-order disturbance observer	3. Differential neural network observer	3. Proportional-SMO
4. High-gain observer	4. Asymptotic observer (AO)	4. Ensemble Kalman filter (EnKF)	4. Bode-ideal cut-off observer	4. EKF with neural network model	4. Continuous-discrete observer
5. Zeitz nonlinear observer	5. Exponential observer	5. Steady state Kalman filter (SSKF)	5. Unknown input observer (UIO)		5. Continuous-discreteinterval observer
6. Discrete-time nonlinear recursive observer (DNRO)	6. Integral observer	6. Adaptive fading Kalman filtering (AFKF)	6. Nonlinear unknown input observer		6. Continuous-discreteEKF

7. Geometric observer	7. Interval observer	7. Moving horizon estimator (MHE)	7. Extended unknown input observer		7. High-gaincontinuous-discrete
8. Backstepping observer		8. Generic observer	8. Modified proportional observer		
		9. Specific observer			

In current thesis, an Artificial intelligence-based observer was developed. In [52] the authors built bioprocess model using ANN. The authors considered two cases; the first one is a common industrial application that is the fed-batch penicillin fermentation. The second case is continuous mycelium fermentation. Both systems serve to demonstrate the utility, flexibility and potential of the artificial neural network approach to process modelling.

In [53] the authors proposed ANN techniques for modeling of the microbial production of PHB by *Azohydromonas lata* as function of the glucose concentration and CDW getting a good approximation to experimental data and a low Minimum Mean Square Error (MMSE).

Artificial Neuronal Networks (ANN) are very useful for approximating the complex nonlinear relationships with less a prior knowledge of the model structure [54], [55] [59] This method develops mathematical algorithms derived from artificial intelligence techniques that try to model the present understanding of human brain. ANN models are proposed in this work for on-line estimation of the Molecular Weight Distribution (MWD) in the fermentation process. The most common structure is feedforward ANN.

2.3.2 Dynamic optimization

Advanced control strategies typically use models (i.e. Phenomenological-Based Semiphysical Models or black box models) in order to predict the dynamic behavior of

the main process variables for choosing the best set of control actions that must be applied in order to optimize a specific objective. The computation of optimal control policies in fed-batch processes requires special effort due to problem characteristics and to the presence of path constraints in the state and control variables. Moreover, adding the possible existence of discontinuities and non-differentiability in the variable profiles and differential equations, a complex dynamic optimization problem is generated, whose solution strategies must be investigated [10].

According to [56] a mathematical description of a dynamic optimization problem (Dopt) is described by Equation 1.

$$\underset{\boldsymbol{u(t)},\boldsymbol{t_f}}{\boldsymbol{min}}\boldsymbol{J}=\underset{\boldsymbol{u(t)},\boldsymbol{t_f}}{\boldsymbol{min}}\left[\emptyset\left(\boldsymbol{X}\left(\boldsymbol{t_f}\right)\right)+\int_{\boldsymbol{t_0}}^{\boldsymbol{t_f}}\boldsymbol{L}(\boldsymbol{X}(\boldsymbol{t}),\boldsymbol{u}(\boldsymbol{t}),\boldsymbol{\theta}(\boldsymbol{t}),\boldsymbol{t})\boldsymbol{dt}\right] \quad \textbf{(1)}$$

s.to

$$\frac{\boldsymbol{dX}}{\boldsymbol{dt}}=\boldsymbol{f}\left(\boldsymbol{X}(\boldsymbol{t}),\boldsymbol{u}(\boldsymbol{t}),\boldsymbol{\theta}(\boldsymbol{t})\right) \quad \textbf{(1a)}$$

$$\boldsymbol{X}(\boldsymbol{t_0})=\boldsymbol{X_0} \quad \textbf{(1b)}$$

$$\boldsymbol{g}\left(\boldsymbol{X}(\boldsymbol{t}),\boldsymbol{u}(\boldsymbol{t}),\boldsymbol{\theta}(\boldsymbol{t})\right)=\boldsymbol{0} \quad \textbf{(1c)}$$

$$\boldsymbol{h}\left(\boldsymbol{X}(\boldsymbol{t}),\boldsymbol{u}(\boldsymbol{t}),\boldsymbol{\theta}(\boldsymbol{t})\right)\leq\boldsymbol{0} \quad \textbf{(1d)}$$

$$\boldsymbol{X^l}\leq\boldsymbol{X}(\boldsymbol{t})\leq\boldsymbol{X^U} \quad \textbf{(1e)}$$

$$\boldsymbol{u^l}\leq\boldsymbol{u}(\boldsymbol{t})\leq\boldsymbol{u^U} \quad \textbf{(1f)}$$

Where $\emptyset\left(\boldsymbol{X}\left(\boldsymbol{t_f}\right)\right)$ is called the Mayer Term, which is related to the state of the process at the final time. Moreover, $\int_{\boldsymbol{t_0}}^{\boldsymbol{t_f}}\boldsymbol{L}(\boldsymbol{X}(\boldsymbol{t}),\boldsymbol{u}(\boldsymbol{t}),\boldsymbol{\theta}(\boldsymbol{t}),\boldsymbol{t})\boldsymbol{dt}$ is called Lagrange Term, and represents an economical function related to the dynamic behavior of the state variables during the transition from the initial optimization time (0) to the final optimization time (t_f).

Based on [56], there exist three types of Dopt solution methods. The first one is Dynamic Programming, which leads to the so-called Hamilton –Jacobi Bellman (HJB) equation, a

partial differential equation (PDE) in the state space. The second approach includes the indirect methods, which uses the necessary conditions of optimality to derive a two-point boundary value problem (BVP). This includes also the calculus of variations, the Euler-Lagrange differential equations, and the so-called Pontryagin Maximum Principle. If the problem requires the handling of active inequality constraints, this kind of methods are usually avoided.

The third approach are the direct methods, which transform the original problem into a finite dimensional nonlinear programming problem (NLP) which is then solved by numerical optimization problems. Methods than apply NLP solvers, can be separated into two groups. First, the sequential approach also called Control Vector Parametrization (CVP) or single shooting, which in Equation 1, only discretizes u(t). The second approach is the so-called simultaneous strategy, which usually uses collocation methods, for discretizing u(t) and X(t) simultaneously.

The sequential methods are relative easy to construct and to apply as they rely on the use of Differential Algebraic Equations (DAE) solvers as well as NLP solvers. Repeated numerical integration of the DAE model is required, which may become time consuming for large-scale problems. On the other hand, in the simultaneous methods, the use of collocation or multiple shooting results in larger NLP problems with junction constraints to handle the system dynamics, which requires the use of specific optimization methods and may be computationally intensive for large-scale dynamic system.

According to [57], dynamic optimization allows the computation of the optimal operating policies in order to get the best time-varying feed rate(s) which ensure the maximization of a pre-defined performance index (usually, a productivity, or an economical index derived from the operation profile and the final concentrations). Once computed in a reliable way, these operating policies can be implemented using different control strategies, such as adaptive control, model predictive control or optimizing control.

The authors in [57], proposed that the general dynamic optimization (optimal control) problem of a bioprocess, considering a free terminal time, can be stated as finding the control vector and the final time to minimize (or maximize) a performance index. In order to surmount these difficulties, the authors presented several alternatives; stochastic and hybrid techniques based on the CVP approach. As it was mentioned before, the CVP approach is a direct method, which transforms the original problem into a NLP problem, which must be solved by a suitable (efficient and robust) solver. However, in [43], the author presented a smoothest alternative than CVP called sinusoidal parameterization, that lies with the feeding polices avoiding inhibitory terms due the strong changes in substrates concentration.

3. MODELLING OF THE PHA´s FERMENTATION PROCESS

In this chapter, the different Phenomenological-Based Semiphysical Models (PBSM) used on the development of this work for describing the fermentation stage on the polyhydroxyalkanoates production are presented. First, a batch model of the process describing the dynamic behavior of biomass, polymer, carbon and nitrogen sources, dissolved oxygen and carbon dioxide is shown. Then, extension of this model is carried out for formulating a fed-batch process model. Finally, a polymerization/kinetic model is described, which is useful for obtaining the dynamic data of Mn and Mw for building, training and validating an ANN in section 3.5

3.1. Batch model

The batch model was developed taking as a base the works by [58], [18]. The following assumptions are considered:

- ✓ A Monod-Sigmoidal expression with uncompetitive substrate limitation and oxygen limitation is used for biomass growth rate.
- ✓ It is expected that production of product will vary dependently of biomass generation and it will not compete for energy resources. The system is analyzed macroscopically (No discretization of elements that exist in it).
- ✓ Biomass (R) is composed of two components: i) The catalytically active component consists of proteins and nucleic acids (X), and ii) Product PHA (P) is an inert component
- ✓ Nitrogen is the limiting nutrient affecting the PHA production in a complex manner.
- ✓ Good control of temperature and pH (30°C and 7) on the set values is reached.
- ✓ The culture media is perfectly mixed, it is assumed that a small portion of the fermentation broth is exactly equal to a different portion, also considered homogeneous system (the same phase).

- ✓ The inoculum corresponds to the exponential part of the growth of the strain.

The Model (based on the work by [41]) is described by Equations (2-8), where the dynamic equations describing the behavior of the state variables biomass (X), substrate (S), product (P), nitrogen-source (N), dissolved oxygen (O_2L) and carbon dioxide (CO_2) concentrations. The specific growth rate (μ) depends of the substrate concentration (S), nitrogen-source concentration (N) and Oxygen concentration (O_2), following a sigmoidal relationship [38], [46]. Equation 2 describes the biomass specific growth rate. This equation is proposed in this work for taking into account the effect of the ratio of nitrogen and carbon source and the limitation in dissolved oxygen based in work presented in [17].

$$\mu = \mu_m \left(\frac{\left(\frac{N}{S}\right)}{\left(\frac{N}{S}\right)+K_{sr}} \right) * \left(1 - \left(\frac{\frac{N}{S}}{S_m} \right)^{n_k} \right) * \left(\left(\frac{O_2L}{K_{ox}*X+O_2L} \right) \right) \quad (2)$$

$$\dot{X} = \mu X \quad (3)$$

$$\dot{S} = -\Big((C_{sx}\, \mu X) + (R_{csx}X) + C_{sp}\big((K_1\, \mu X) + (K_2X) \big) \Big) \quad (4)$$

$$\dot{P} = (K_1 \mu X) + (K_2X) \quad (5)$$

$$\dot{N} = -\big((C_{nx}\ \mu\ X) + (R_{cnx}\ X) \big) \quad (6)$$

$$\dot{O_2L} = ((KL(O_{2Leq} - O_2L)) - (K_3\, \mu X) - ((K_4K_1\, \mu X) + (K_4K_2X))) \quad (7)$$

$$\dot{CO_2} = (\alpha_1\mu + \alpha_2)X + \alpha_3 \quad (8)$$

Table 6 shows the nomenclature used in Equations (2-8). The model contains 19 parameters. For identifying those parameters, a hybrid strategy combining the simulated annealing optimization algorithm and the interior point method was used, as suggested in [18]. The minimization criteria for parameter identification used was:

$$\boldsymbol{SSWR} = \sum_{i=1}^{n} \sum_{j=1}^{m} \frac{\Delta_{ij}}{W_i^2} \quad . \quad (9)$$

Where:

- SSWR represents the sum of the square of weighed residuals,
- 'i' and 'j' are the number of experimental data points and number of variables, respectively,
- 'n' and 'm' are the total number of experimental data points and total number of variables, respectively,
- W_j is a normalization factor for each variable (i.e. the maximum value of each variable), and
- Δ_{ij} is the difference between the predicted values by the model and the experimental data ($y_{model} - y_{expt}$).

The experimental data for identification and validation were taken from [58]; the optimized model parameters are shown in Table 6.

Table 6 Parameters for the Batch process Model

Parameter	Seed Value	Optimal Value	Re-optimized value	Meaning (Units)
μ_m	0.54	0.42	0.61	Maximum specific growth rate h^{-1}
K_{sr}	0.15	0.015	0.015	Saturation Constant (g/L)
S_m	0.3	3.7	5.2	Maximum Value of substrate at which μ is zero (gN/L /gS/L)
C_{sx}	1.76	1.18	1.37	Yield of substrate respect to biomass gS/gX
R_{csx}	0.022	$1.64*10^{-4}$	$7.55*10^{-5}$	Consumption Rate (gS/gXh)
C_{sp}	1.75	0.0039	0.0039	Yield of substrate respect to product (gS/gP)
k_1	0.14	0.36	0.35	Yield of product respect to biomass (gP/gX)
k_2	0.74	0.006	0.006	Consumption rate (gP/gXh)
C_{nx}	0.336	0.0096	0.0096	Consumption rate (gN/gNh)
KL	0.1	0.62	0.62	Aeration constant (L/h)
k_3	93	191.3	191.3	Yield of oxygen respect to biomass

				(gO_2/gX)
k_4	85	77.25	77.25	Yield of oxygen respect to Product (gO_2/gP)
O_{2Leq}	0.0076	0.0066	0.0066	Dissolved Oxygen in saturation stage (g/L)
n_k	1.22	9.85	21.6	Exponent on the equation (1)
R_{cnx}	0.16	0.0017	0.0014	Consumption rate (g/gh)
α_1	0.143	0.75	0.75	Constant for CO_2 with growth ($mmolCO_2/gX$)
α_2	$4*10^{-7}$	$2.13*10^{-6}$	$2.13*10^{-6}$	Constant for CO_2 with maintenance energy ($mmolCO_2/gXh$)
α_3	$1*10^{-4}$	$6.84*10^{-4}$	$6.84*10^{-4}$	Constant for CO_2 with product ($mmolCO_2/Lh$)
K_{ox}	0.02	$7.9*10^{-4}$	$7.9*10^{-4}$	Yield of oxygen respect to biomass in μ (gO_2/gX)

Figure 3 shows the simulation results for the main states variables and for the specific growth rate. Such results are named as Model identification, meaning that those model predictions were obtained after parameter identification (i.e. performed by solving the optimization problem for the objective function described by equation (9)). The obtained parameters are listed on column 3 of table 6. The dissolved oxygen concentration was kept constant at 40% of saturation, as suggested in the literature [58], [18].

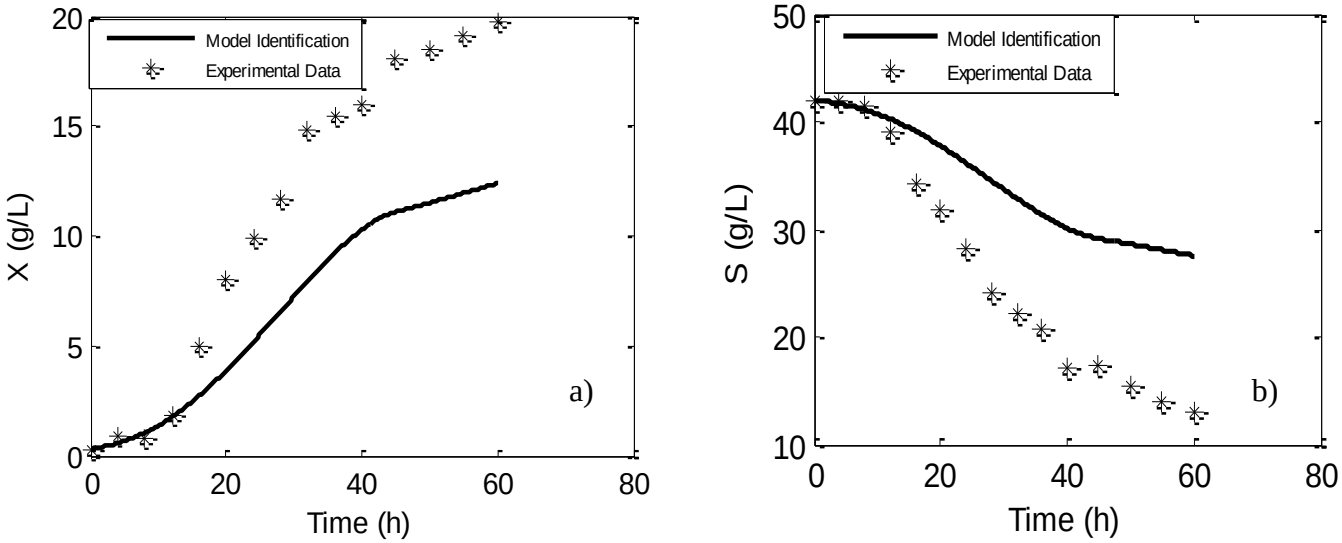

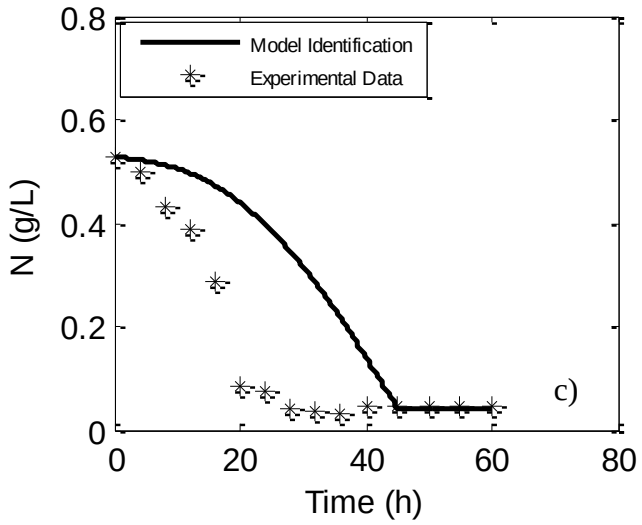
Model Identification
Experimental Data
N (g/L)
Time (h)
c)

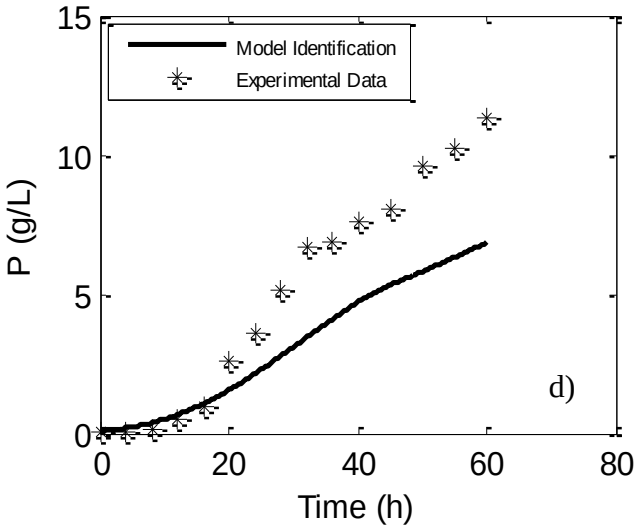
Model Identification
Experimental Data
P (g/L)
Time (h)
d)

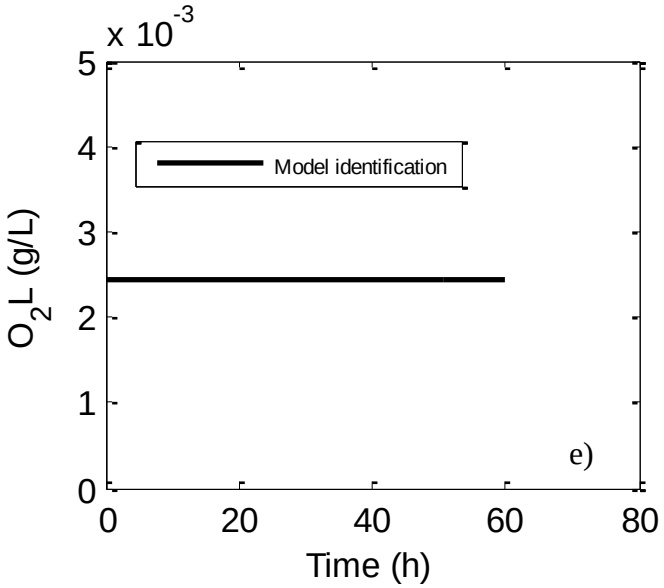
x 10-3
Model identification
O2L (g/L)
Time (h)
e)

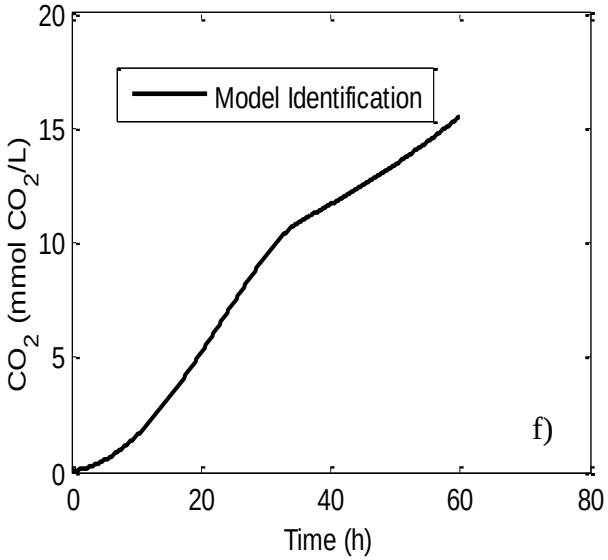
Model Identification
CO2 (mmol CO2/L)
Time (h)
f)

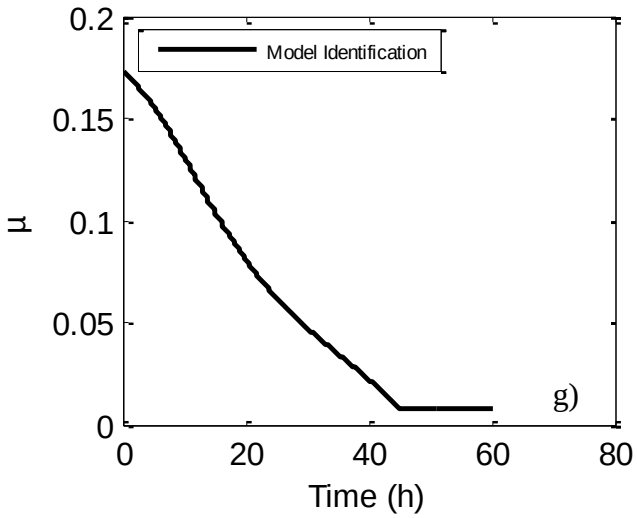

Figure 3 Simulation of different Dynamics. a) Biomass, b) Carbon source, c) Polymer, d) Nitrogen source, e) Dissolved Oxygen, f) Dissolved Carbon dioxide, g) Specific Growth Rate.

As it can be seen from Figures 3a) to 3d), the parameter identification need to be improved, since there are still important deviations between the model predictions and the experimental data. In the next section a re-optimization strategy as suggested by [59] is carried out towards finding the set of most sensitive parameters that should be re-optimized, in order to improve the parameter identification and therefore, the model fit.

3.2. Re-optimization strategy.

First, sensitivity analysis is carried out in order to determine the most sensitive parameters affecting the objective function (i.e. the residuals for the main state variables). Then, the most sensitive parameters are re-optimized, using the set of validation data, whereas the remaining parameters are kept fixed at their original values (i.e. the shown in the third column at Table 6).

3.2.1. Sensitivity Analysis

In order to get the most sensitive parameters, both, a global as well as a relative sensitivity analysis were carried out. The first one is related to the prediction error, whereas the latter to analyze the influence of each parameter on each state variable. In both cases, sensitivity was tested for a variation of ±10% in the value of each parameter. Figure 4 shows the results for the global sensitivity analysis, where the %Error is the deviation of the optimal value. According to the results, from the set of 19 parameters, the most sensitive parameters are S_m, μ_m, C_{sx}, R_{csx}, k_1, n_k and R_{cnx}.

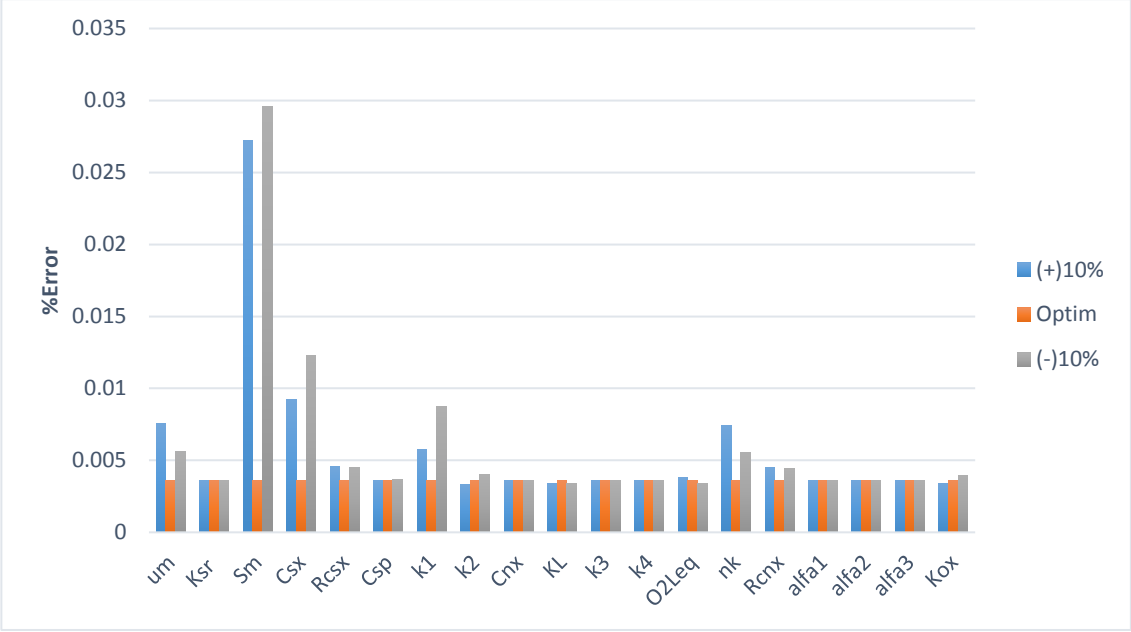

Figure 4 Global Sensitivity analysis.

The relative sensitivity analysis per state variable is carried out in the following [9]. In a general formulation, a state space model can be written as:

$$\dot{\boldsymbol{\varepsilon}} = \emptyset(\boldsymbol{\varepsilon}, \boldsymbol{\theta}, \boldsymbol{\mu}) \tag{10}$$

where $\emptyset$ is function of the states ($\boldsymbol{\varepsilon}$), parameters ($\boldsymbol{\theta}$) and feed flow rates ($\boldsymbol{\mu}$) for the fed-batch and continuous cases.

In [9] the relative sensitivity function, which finds the change of each state variable with respect to each parameter, is given by:

$$\boldsymbol{S}_{\boldsymbol{\theta}_j}^{\boldsymbol{\varepsilon}_i} = \left(\frac{\boldsymbol{\partial \varepsilon_i}}{\boldsymbol{\partial \theta_j}}\right)\frac{\boldsymbol{\theta_j^*}}{\boldsymbol{\varepsilon_i^*}} \tag{11}$$

Where for our specific problem, $i = 1, \ldots, 6$. $j = 1, \ldots, 19$. Using a central finite differences approximation, Equation (11) becomes,

$$\boldsymbol{S}_{\boldsymbol{\theta_1}}^{\boldsymbol{\varepsilon_1}} = \left(\frac{\boldsymbol{\partial \varepsilon_1}}{\boldsymbol{\partial \theta_1}}\right)\frac{\boldsymbol{\theta_1^*}}{\boldsymbol{\varepsilon_1^*}} = \left(\frac{\boldsymbol{\varepsilon_1(t,\theta_1+\Delta\theta_1)-\varepsilon_1(t,\theta_1-\Delta\theta_1)}}{\boldsymbol{2\Delta\theta_1}}\right)\frac{\boldsymbol{\theta_1^*}}{\boldsymbol{\varepsilon_1^*}} \tag{12}$$

Figures 5 to 10 show the results for the relative sensitivity analysis of some parameters on the state variables. In conclusion, the relative sensitivity analysis reinforces the results obtained by the global analysis, and therefore, the most sensitive parameters affecting the objective function (i.e. a measurement of model prediction's error) are taken to be S_m, μ_m, C_{sx}, R_{csx}, k_1, n_k and R_{cnx}.

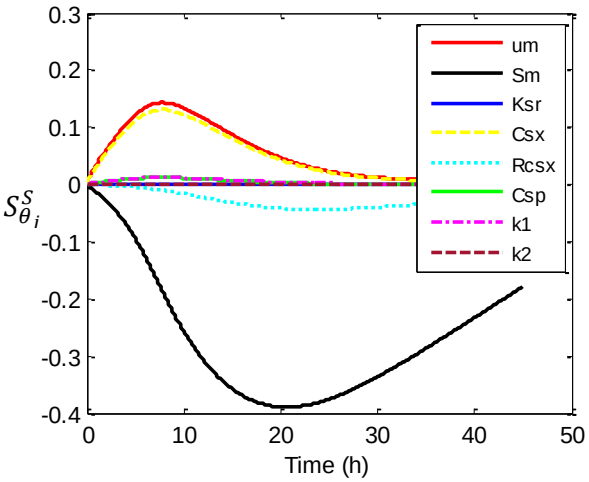

Figure 5 Sensitivity on Substrate concentration

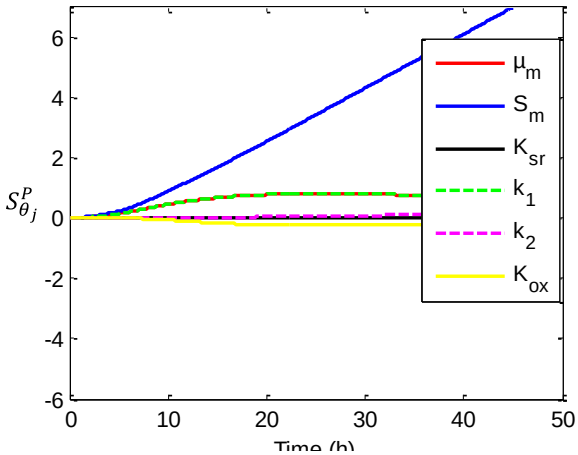

Figure 6 Sensitivity on Polymer concentration

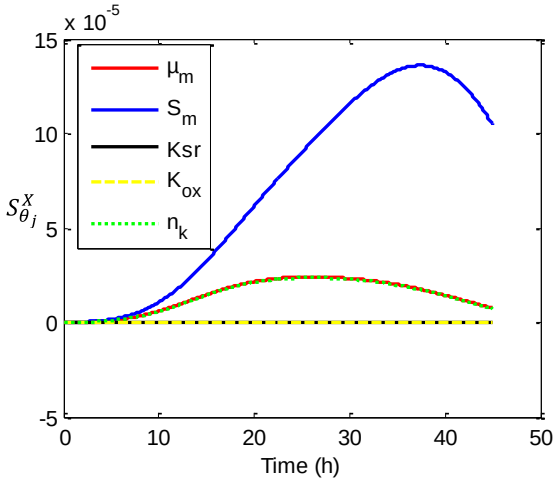

Figure 7 Sensitivity on Biomass

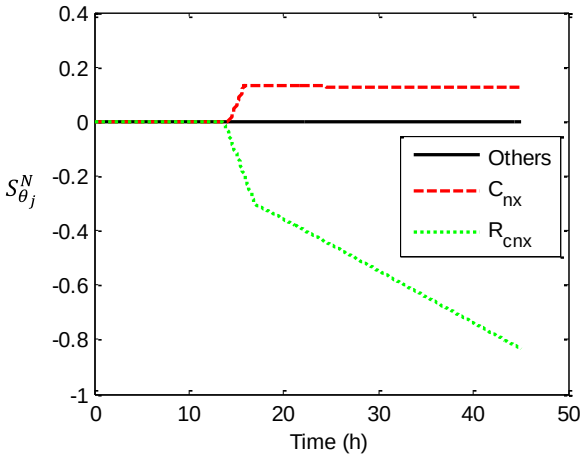

Figure 8 Sensitivity on Nitrogen

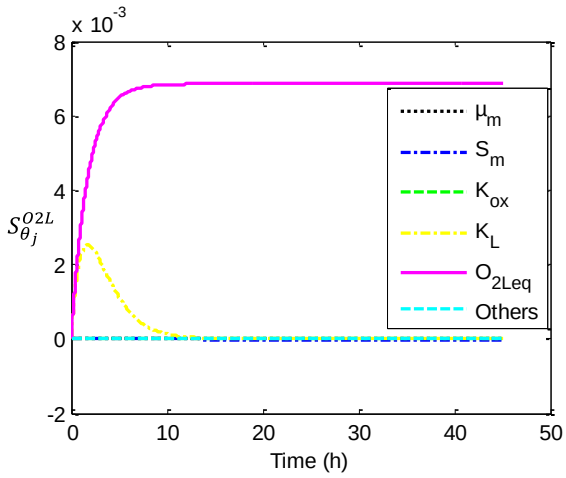

Figure 9 Sensitivity on Dissolved Oxygen Concentration

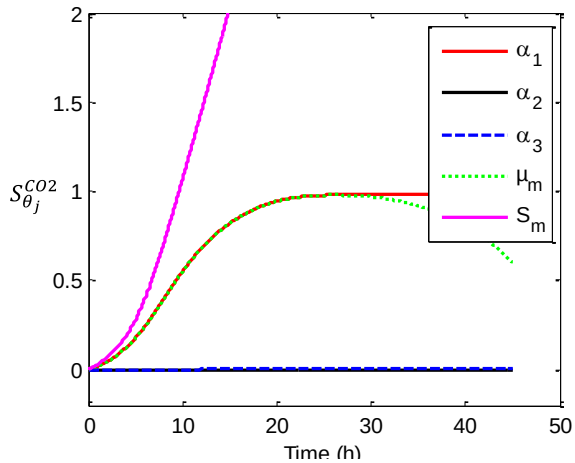

Figure 10 Sensitivity on Carbon Dioxide Concentration

3.2.2. Parameters re-optimization using the validation data

As it was shown, 7 parameters (from the 19 that compose the model) have been identified as the most sensitive. Therefore, the re-optimization strategy is applied towards finding a better value for this set of sensitive parameters, while keeping fixed the remaining 12 parameters (i.e. fixed at the values found previously). For the re-optimization, the same hybrid strategy that for the first identification (simualted annealing + interior point method) was used. Resutls of the re-optimization using the validation data

are shown in Figure 11. In Figures 11-c) and 11-g), it can been observed a lower limit in the carbon source concentration and the specific growth rate, and it was induced using a restriction of the type “If” in order to get a more adecuated behaviour in the states . As it can be seen, model predictions have been improved, and now fit very well the experimental data.

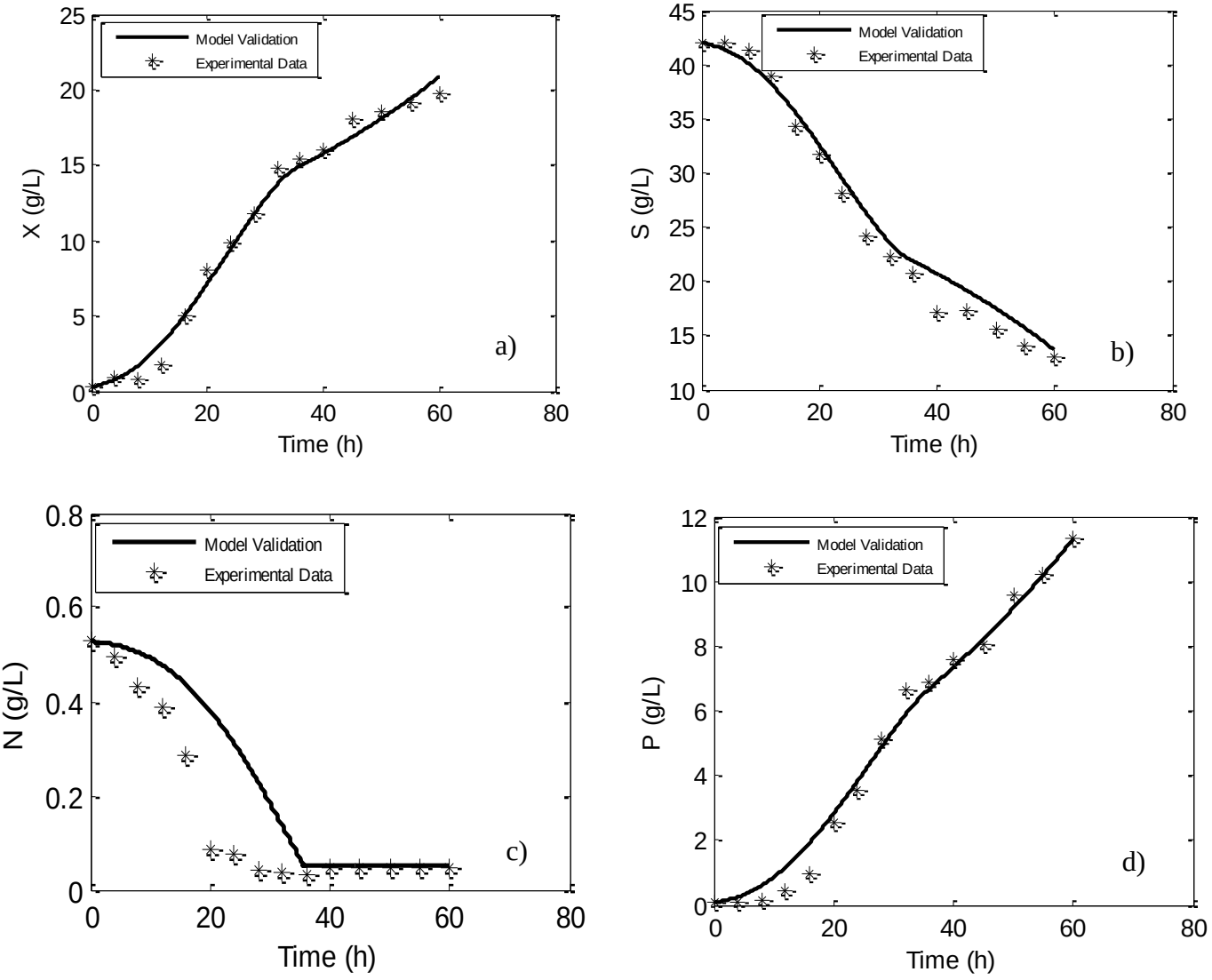

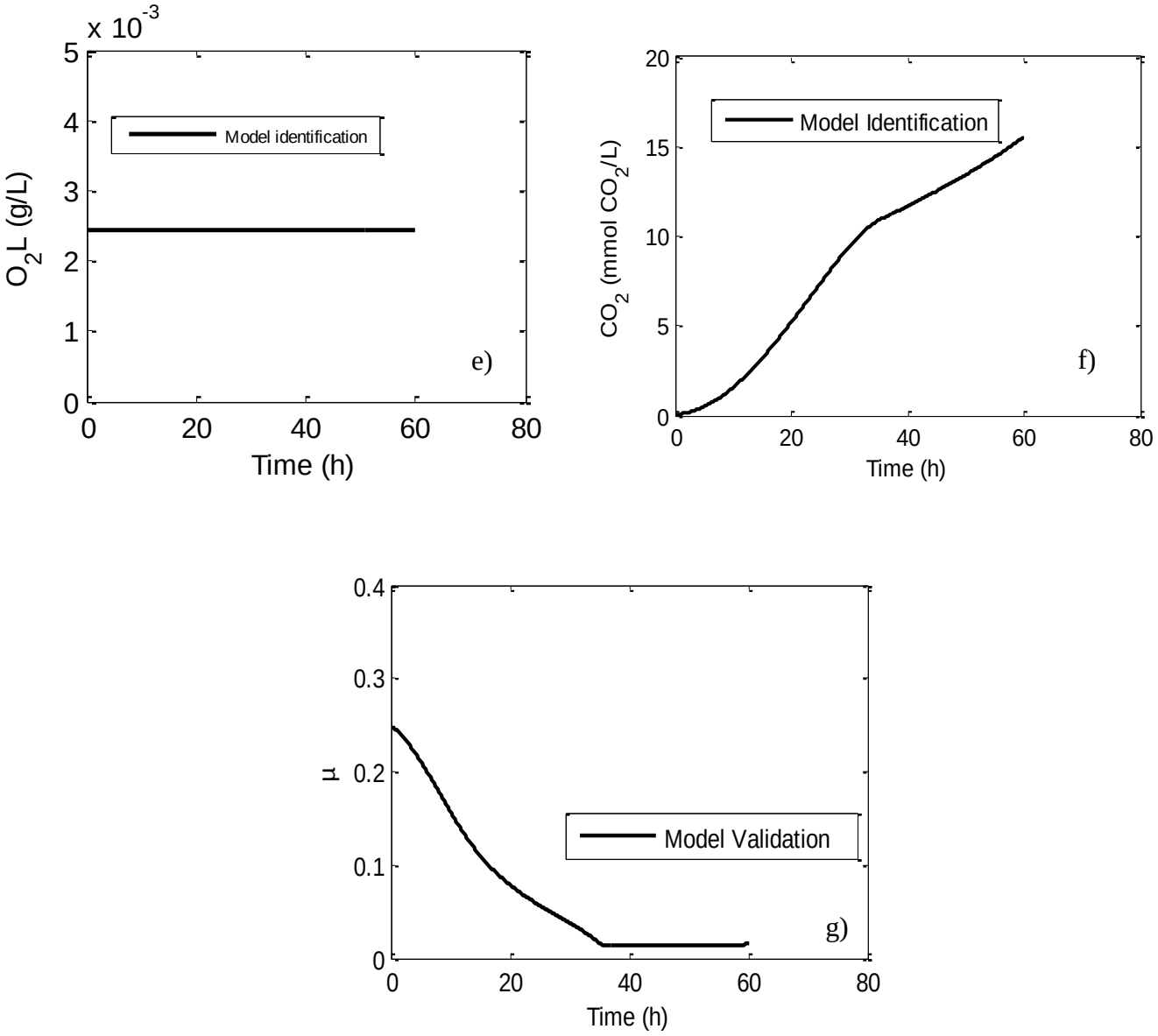

Figure 5 Simulation of different Dynamics. a) Biomass, b) Substrate, c) Polymer, d) Nitrogen, e) Dissolved Oxygen, f) Dissolved Carbon Dioxide , g)Specific Growth Rate.

3.3. Fed-Batch Model

The fed-batch model of the process was developed based on the previous batch model**.** It keeps the same mathematical structure with the addition of the dilution rates and feeding strategy. Equations 13 to 19 represent the fed-batch model, where F_1, F_2 and F_3 (L/h) correspond to the feed flow rates of carbon, nitrogen and oxygen sources respectively. S_{in}, N_{in} and O_{in} correspond to the concentrations of carbon, nitrogen and oxygen sources at F_1, F_2 and F_3, respectively. Finally, V is the fermentation volume.

$$\dot{X} = \mu X - \frac{F_1+F_2}{V} X \tag{13}$$

$$\dot{S} = -\Big((C_{sx}\mu X) + (R_{csx}X) + C_{sp}\big((K_1\mu X) + (K_2 X)\big)\Big) + \frac{F_1}{V} S_{in} - \frac{F_1+F_2}{V} S \tag{14}$$

$$\dot{P} = (K_1 \mu X) + (K_2 X) - \frac{F_1+F_2}{V} P \tag{15}$$

$$\dot{N} = -\big((C_{nx}\ \mu\ X) + (R_{cnx}\ X)\big) + \frac{F_2}{V} N_{in} - \frac{F_1+F_2}{V} N \tag{16}$$

$$\dot{O_2}L = ((KL(O_{2Leq} - O_2 L)) - (K_3 \mu X) - ((K_4 K_1 \mu X) + \ (K_4 K_2 X))) + \frac{F_3}{V} O_{in} - \frac{F_1+F_2}{V} O_2 L \tag{17}$$

$$\dot{CO_2} = (\alpha_1 \mu + \alpha_2) X + \alpha_3 - \frac{F_1+F_2}{V} CO_2 \tag{18}$$

$$\dot{V} = F_1 + F_2 \tag{19}$$

The experimental data, modelling conditions and the feeding strategy for validating the fed-batch model were taken from [18]; the parameter adjustment was done in a similar way as described in section 3.2. Figure 12 shows the model predictions (i.e. Model validation) against the experimental data for the feeding policy in Figure 12-h). It can be observed that the model fitting has a good approximation to the experimental data. The pulse feeding strategy is one of the most important strategies in bioprocess, but, in section 4.1 it will be analyzed other common strategies.

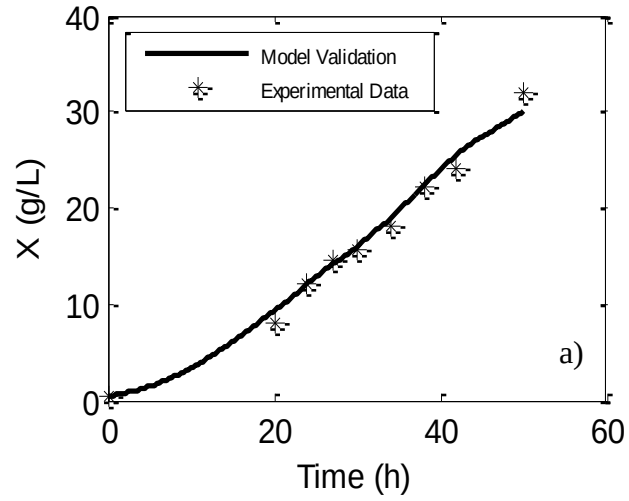
Model Validation
Experimental Data
X (g/L)
Time (h)
a)

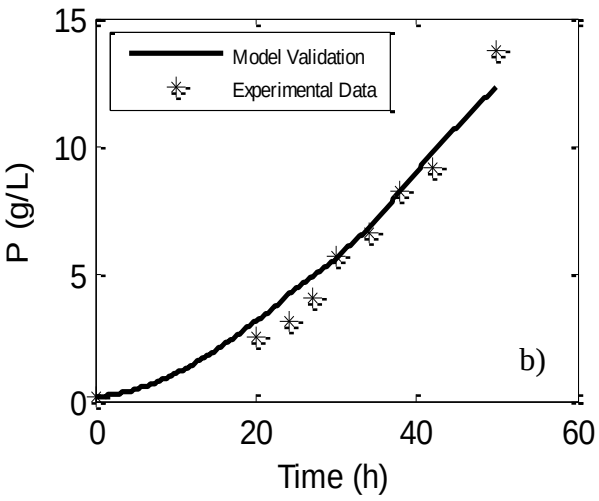
Model Validation
Experimental Data
P (g/L)
Time (h)
b)

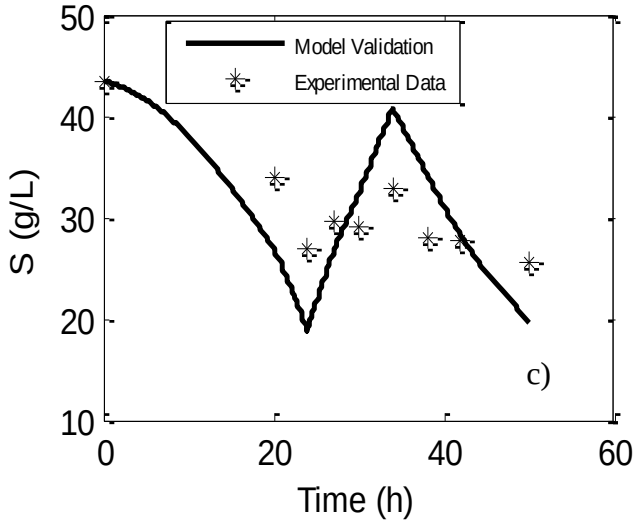
Model Validation
Experimental Data
S (g/L)
Time (h)
c)

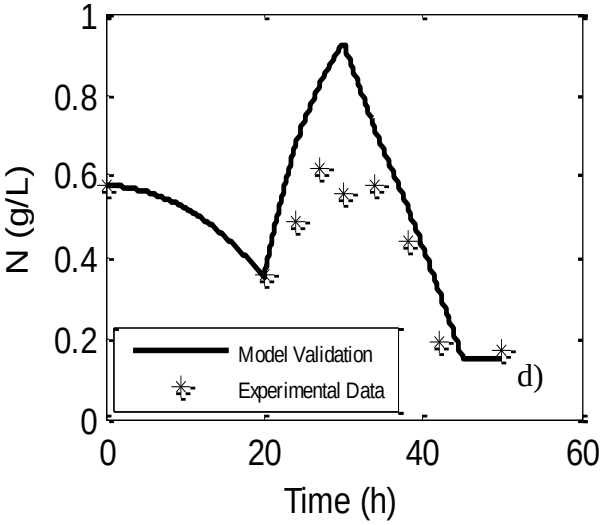
Model Validation
Experimental Data
N (g/L)
Time (h)
d)

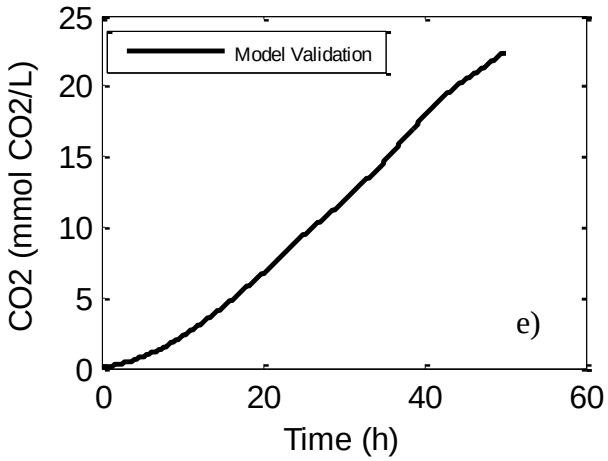
Model Validation
CO2 (mmol CO2/L)
Time (h)
e)

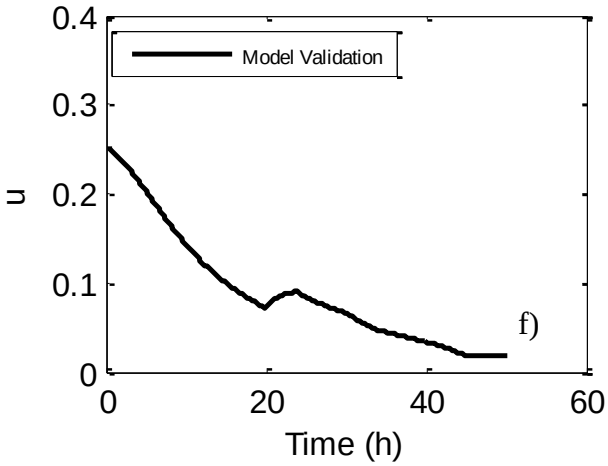
Model Validation
u
Time (h)
f)

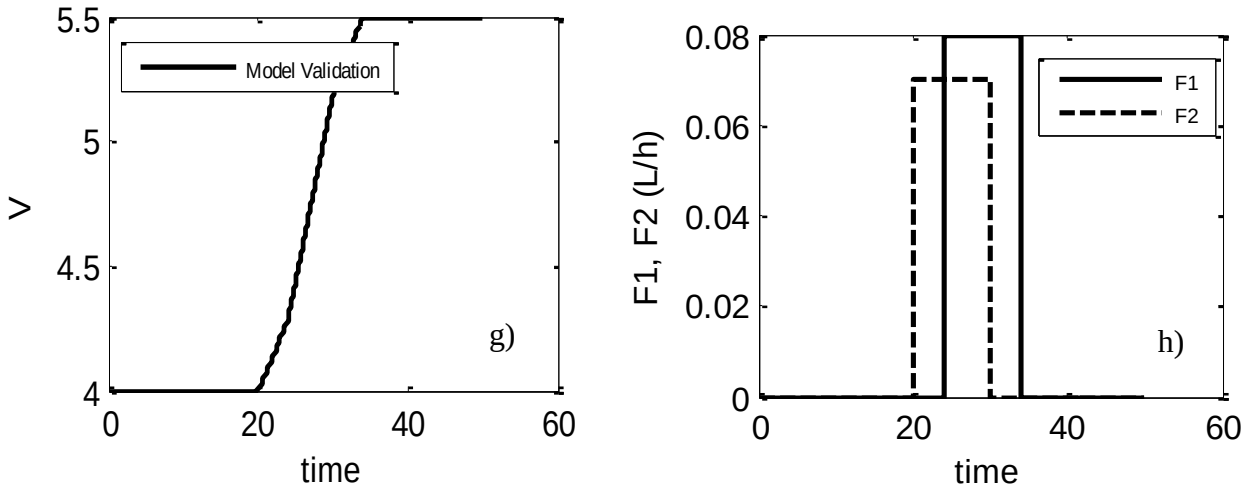

Figure 6 Simulation of different fed-batch Dynamics a) Biomass, b) Polymer, c) Carbon source, d) Nitrogen Source, e) Dissolved Carbon Dioxide, f) Specific Growth rate, g) Fermentation Volume and h) Feeding Strategy.

3.3.1. Fed Batch sensitivity analysis

A sensitivity analysis for the fed-batch process was carried out in order to analyze the effect of the initial conditions, feeding strategy and feed concentrations into a profitability function.

The set of ordinary differential equations (13-19) can be expressed as a vector of seven components, where i, corresponds to the number of the states described before $[X, S, P, N, O_2L, CO_2, V]$:

$$\frac{dx}{dt} = f(x, F) \tag{20}$$

Initial conditions: $x_i(0)$ $i = 1, 2, \ldots, 7$:

$$\boldsymbol{x_{min,i} \leq x_i(0) \leq x_{max,i},\ i = 1, 2, \dots, 7} \quad (21)$$

The state vector x is an (7x1) vector and F is an (2x1) control vector bounded by

$$\boldsymbol{F_{min,j} \leq F_j \leq F_{max,j},\ j = 1, 2} \quad (22)$$

The objective is to maximize the profitability function ($\boldsymbol{P_F}$). The decision variables are the substrates and feed initial concentrations and feed flow rates for carbon and nitrogen sources. The constraints values were taken based on [60] in inhibition conditions for that specific case of 4 Lts fermentation.

$$\underset{F_i(t), xi(0), xi\ in}{Maximize}\ P_F \quad (23)$$

s.to

$$0.02 \leq F_j \leq 0.1, \left(\frac{L}{h}\right)\ i = 1,2 \quad (23a)$$

$$10 \leq x_2(0) \leq 100, \left(\frac{g}{L}\right) \quad (23b)$$

$$0.22 \leq x_4(0) \leq 1.2, \left(\frac{g}{L}\right) \quad (23c)$$

$$150 \leq x_{2in} \leq 600, \left(\frac{g}{L}\right) \quad (23d)$$

$$6.3 \leq x_{4in} \leq 70, \left(\frac{g}{L}\right) \quad (23e)$$

$$x_7 \leq 7L \quad (23f)$$

The profitability function was defined according to [61], [62], [63], [64]. In equation 24, is defined the profitability function that is used to solve the Equation 23. In Table 7 are the values of the main profitability variables in order to get a solution of Equation 23.

$$P_F = (PHB * V * G) - V * \{R1 * S0 + R2 * N0\} - ti * \{M1 * F1 + M2 * F2\} - [EP * ti] \quad (24)$$

Where G, R1 , R2, ti, M1, M2 and EP are raw polymer price, cost of the initial carbon source concentration, cost of the initial nitrogen source concentration, fermentation time, cost of feeding carbon source, cost of feeding nitrogen source and operational and energetic cost respectively.

Table 7 Profitability Variables

Variable	Amount/cost (USD)
G($/g)	1.45
R1($/g)	0.7
R2($/g)	0.25
ti(h)	50
M1($/L)	0.8
M2($/L)	0.33
EP($/h)	1.1

Based in the economic information, an equilibrium point evaluation was performed taking into account the minimal polymer production required in order to reach the zero point with the revenue and costs. It was built based in the information described above and it was a simple calculation in order to determine the minimal production.

Figure 13 shows that the minimal production should be at least 20 g/l of polymer. Based on this result, the optimal initial conditions for the fed-batch fermentation were found, as it is shown in Table 8.

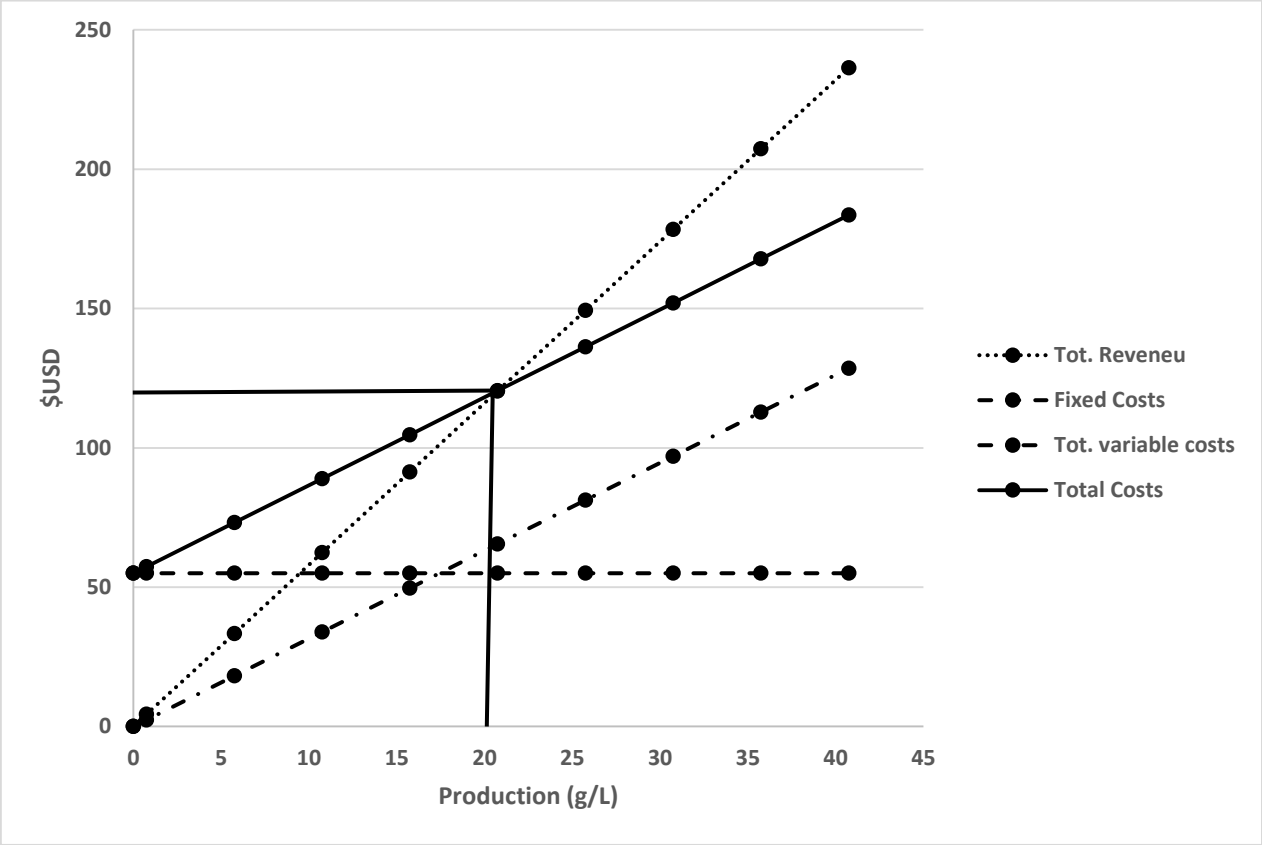

Figure 7 Equilibrium point for the function cost

Table 8 Optimal Fermentation Conditions for the Fed-batch process obtained by Equation (23).

Variable/Value						Final Polymer (g/L)	Profitability $USD
N_0 (g/L)	S_0 (g/L)	F_1 (L/h)	F_2 (L/h)	S_{in} (g/L)	N_{in} (g/L)	**26**	**30.27**
0.87	21.75	0.092	0.06	600	61.8		

As it is shown in Table 8, productivity is related with the profitability; so, it is important for real case applications, to ensure the obtention of a high amount of polymer, but with desired end-product specifications (i.e. Molecular weight, polydispersity index). This is precisely the reason that makes necessary to develop a control strategy that allows

reaching a high value in polymer concentration, with the required properties, in order to assure the profitability of the biopolymers production.

3.4. Structured kinetic/Polymerization Model

As was mentioned before, the Molecular Weight Distribution (MWD) is a fundamental polymer property that directly influences many of the characteristics of the product, such as its mechanical properties. Maintaining the instantaneous molecular weight constant during the polymerization process allows narrowing the final cumulative MWD, which influences stress–strain properties, stress crack resistance, impact resistance, and thermal properties of many polymer systems [65]. Furthermore, the weight average molecular weight (Mw) influences also the melt and concentrated solution viscosity. Therefore, developing strategies for monitoring and control the molecular weight and the MWD is still a very important industrial issue. Based on the reported works in [38], [46] a macroscopic/polymerization kinetic model was simulated and validated in order to be used for obtaining “in silico” data. Such in silico data are then used for building a soft sensor capable to predict the MW and MWD on-line.

3.4.1. Batch: Structured kinetic/Polymerization Model

The polymerization–depolymerization kinetic scheme is given in the following works [38], [66] and [67]. The polymerization–depolymerization kinetic scheme is as follow:

Initiation:

$$\text{E-SH+M}^{\#} \rightarrow \text{E-SH-M}^{\#} \xrightarrow{k_i} P_1 - ES + CoA - SH \qquad (25)$$

Propagation:

$$P_n - \text{ES+M}^{\#} \xrightarrow{k_{m2}} P_n\text{-ES-M}^{\#} \xrightarrow{k_p} \boldsymbol{P_{n+1}} - ES + CoA - SH \qquad (26)$$

Chain Transfer:

$$P_n - \text{ES} + H_2O \xrightarrow{k_t} D_n + \text{E-SH} \quad (27)$$

Degradation:

$$D_n + \text{E-OH} \xrightarrow{k_d} D_{n-1} + D_1 + \text{E-OH} \quad (28)$$

Where E-SH, $M^{\#}$, CoA-SH and E-OH denote the concentration of shynthase dimer, monomer coenzyme A complex (M-SCoA), coenzyme A and depolymerase, respectively. Besides, $P_n - \text{ES}$ (P_n), P_n-ES-$M^{\#}$ (P_n^*), and D_n are the corresponding concentrations of active, intermediate and inactive polymer chains with a degree of polymerization equal to n.

The mathematical model of set of reactions (25-28) is as follow:

Assumptions:

- Initiation is assumed to occur in two steps with the formation of an intermediate 'synthase–monomer' complex (E-SH+$M^{\#}$).
- A two-step reaction is also considered for polymer chain propagation where an intermediate 'active polymer–monomer' complex (P_n-ES-$M^{\#}$).
- It is assumed that the polymerase (PhaC), depolymerase (PhaZ) and chain transfer agent concentrations are constant throughout the course of polymerization.
- It is considered that the rate-limiting step in the degradation mechanism is the binding of the inactive polymer chain to depolymerase.
- The effects of population heterogeneity (i.e. segregation of cells) and mass-transfer limitation phenomena are not taken into account [38].

The mathematical kinetic/polymerization model for the PHAs production, based on the reaction scheme (25-28), and the mentioned assumptions the net production rates for the various intracellular molecular species, following equations (29-33):

Active Polymer Chains of length "n"

$$\frac{d[P_n]}{dt} = k_i[E-SH-M^{\#}]d(n-1) - k_{m2}[P_n][M^{\#}] + k_p[P^*_{n-1}]H(n-1) - k_t^*[P_n] \quad (29)$$

n=1,2…∞

Intermediate polymer chains of length "n"

$$\frac{d[P^*_n]}{dt} = k_{m2}[P_n][M^{\#}] - k_p[P^*_n] \quad \text{n=1,2…}\infty \quad (30)$$

Inactive polymer chains of length ''n''

$$\frac{d[D_n]}{dt} = k_t^*[P_n] - k_d^*[D_n] + k_d^*[D_{n+1}] \quad \text{n=1,2…}\infty \quad (31)$$

Monomer

$$\frac{d[M^{\#}]}{dt} = J_M(t) - k^*_{m1}[M^{\#}] + k^*_{m2}[M^{\#}]\sum_{n=1}^{\infty}[P_n] \quad (32)$$

Synthase–Monomer complex

$$\frac{d[E-SH-M^{\#}]}{dt} = k^*_{m1}[M^{\#}] - k_i[E-SH-M^{\#}] \quad (33)$$

Where $k^*_{m1} = k_{m1}[E-SH]$, $k_d^* = k_d[E-SH]$ and $k_t^* = k_t[H_2O]$. The Kronecker delta function, d(x), and the Heaviside step function, H(x), are defined by the following equations:

$$d(x) = \begin{cases} 1, if\ x = 0 \\ 0,\ otherwise \end{cases} \quad (34)$$

$$\mathrm{H}(x) = \begin{cases} 1, if\ x > 0 \\ 0, if\ x \leq 0 \end{cases} \quad (35)$$

An important term on the model that deserves special attention is the term $J_M(t)$, which corresponds to the monomer production rate (flux) from upstream metabolic steps. This term is important because it would be used for linking the macroscopic model with the polymerization model, as it is shown in Figure 14.

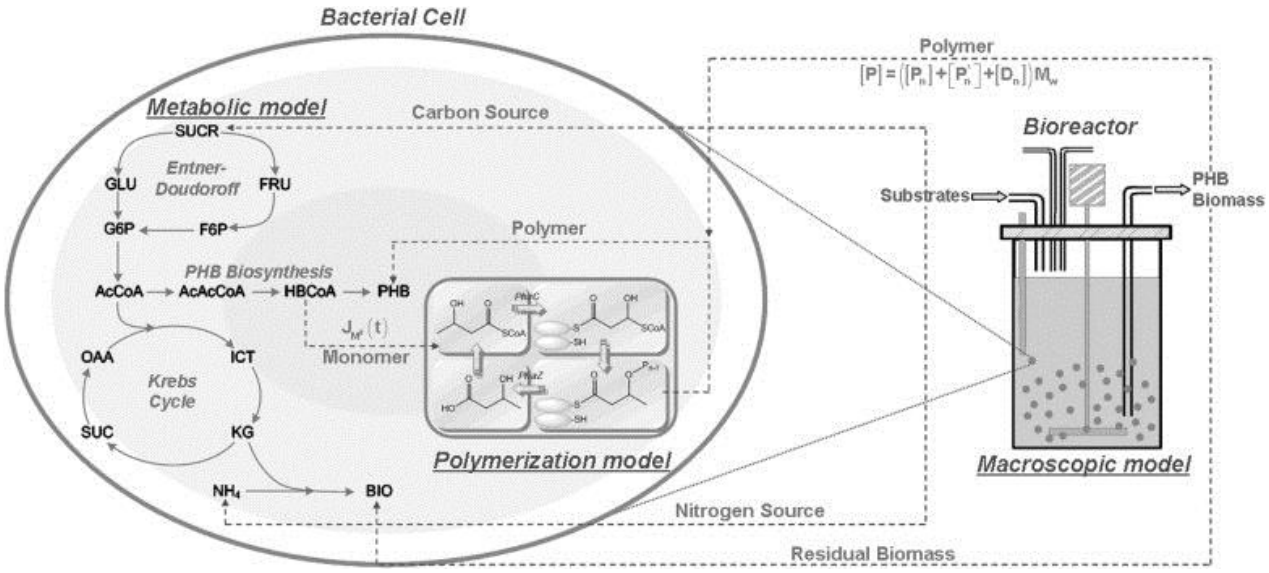

Figure 8 Metabolic/Polymerization and Macroscopic Model [46].

Finding $J_M(t)$ is not a straightforward task. In the following some recommendations given by Dr.Giannis Penloglou [68], on how to calculate $J_M(t)$ are given.

“The first approach is to calculate the monomer concentration via the consumption rate of the substrate. A simple production yield can be used and calculated along with the remaining kinetic constants through the parameter estimation algorithm. This is the simplest approach”.

“The second approach is to integrate the kinetic model with a macroscopic one and define an additional equation based on the total polymer concentration. This equation will allow to estimate an extra unknown, which is the monomer concentration”.

“The third approach is to solve a complete metabolic flux analysis problem that can provide with the concentration of every intracellular metabolite, thus the monomer concentration. It is a more demanding solution, since it will need to know the complete metabolic pathway and the stoichiometry of the reactions. Moreover, it will have to utilize experimental measurements for biomass, substrate, polymer, nitrogen, O_2 and CO_2 concentrations. The solution is based on steady state conditions, thus it will need to solve the flux analysis in every time-point of the experimental measurements”.

For the sake of simplicity, the first approach suggested was used in order to determine $J_M(t)$. On the other hand, numerical solution of the system of equations (29-33) requires the use of specific techniques. In this work, the so-called Fixed Pivot Technique described in [38], [66], [67], was used in order to discretize the set of equations.

3.4.2. Fixed Pivot Technique

The model was simulated and validated using the conditions given in [38]. According to the literature, the maximum degree of polymerization usually lies in the range of 10^6 to 10^7. Equations (29-31) are discretized into (36-38) [46].

Lumped molar balance equations for the ‘active’ polymer chains

$$\frac{\overline{dP}_j}{dt} = k_i[E - SH - M^{\#}]d(j-1) - k_{m2}\bar{P}_j[M^{\#}] + k_P H(j-1)\sum_{k=1}^{j}\bar{P}_k^* A_{j,k} - k_t^*\bar{P}_j \qquad (36)$$

$$j = 1,2,..,nt$$

Lumped molar balance equations for the 'intermediate' polymer chains

$$\frac{d\bar{P}_j^*}{dt} = k_{m2}\bar{P}_j[M^\#] - k_p\bar{P}_j[M^\#] + k_P\bar{P}_j^* \qquad j = 1,2,..,\infty \tag{37}$$

Lumped molar balance equations for the 'inactive' polymer chains

$$\frac{\overline{dD}_j}{dt} = k_t^*\bar{P}_j - k_d\bar{D}_j + k_d^*\sum_{k=j}^{j+1}\bar{D}_k B_{j,k} \qquad \text{j=1,2,…,nt} \tag{38}$$

The matrices $A_{j,k}$ and $B_{j,k}$ are defined as:

$$A_{j,k} = \begin{cases} \frac{x_{j+1}-xt}{x_{j+1}-x_j} & x_j \le x_t \le x_{j+1} \\ \frac{x_t-x_{j-1}}{x_j-x_{j-1}} & x_{j-1} \le x_t \le x_j \end{cases} \quad where\ x_t = x_k + x_1 \tag{39}$$

$$B_{j,k} = \begin{cases} \frac{x_{j+1}-xt}{x_{j+1}-x_j} & x_j \le x_t \le x_{j+1} \\ \frac{x_t-x_{j-1}}{x_j-x_{j-1}} & x_{j-1} \le x_t \le x_j \end{cases} \quad where\ x_t = x_k - x_1 \tag{40}$$

The total polymer chain length distribution of polymer chains is calculated from the sum of the individual 'active', 'intermediate' and 'inactive' polymer chain distributions:

$$\bar{T}_j = \bar{P}_j + \bar{P}_j^* + \bar{D}_j \tag{41}$$

The number average molecular weight (Mn) and the weight average molecular weight (Mw) are given by:

$$M_n = \left(\frac{\sum_{j=1}^{nt} x_j\bar{T}_j}{\sum_{j=1}^{nt}\bar{T}_j}\right) MW \tag{42}$$

$$M_w = \left(\frac{\sum_{j=1}^{nt} x_j{}^2 \bar{T}_j}{\sum_{j=1}^{nt} x_j \bar{T}_j}\right) MW \quad (43)$$

Where MW is the molecular weight of the repeating unit and for β-hydroxybutyrate is 103.04 g/mol.

Now, according to [38], in the case that the biomass concentration is constant, the monomer production rate, $J_M(t)$ can be assumed to be proportional to the fructose consumption rate, $J_F(t)$:

$$J_M(t) = Y_{\frac{M}{F}}\, J_F(t) \quad (44)$$

Where $Y_{\frac{M}{F}}$, is a monomer to substrate yield coefficient (mol of monomer produced/mol of fructose consumed).

Based on the information of Tables 6 and 9 and with a nt value of 51, Figure 15 compares the model predictions with the experimental data (extracted from [38]). Figure 15-e) deserves special attention, because it shows the validation for the Number average Molecular Weight (Mn), and this is also compared to the approximation obtained by [38], [46]. From this, it can be seen that the model simulation results obtained in this work are in good agreement with the experimental data and with [38] predictions for Mn.

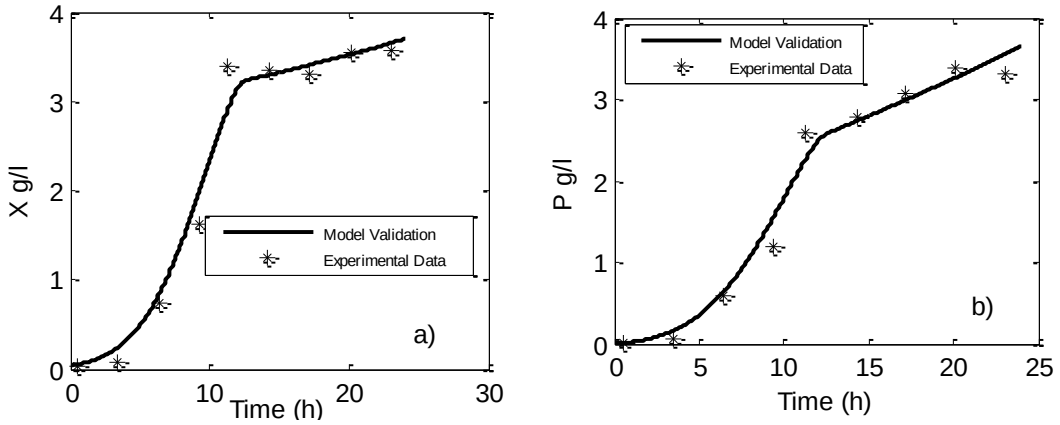

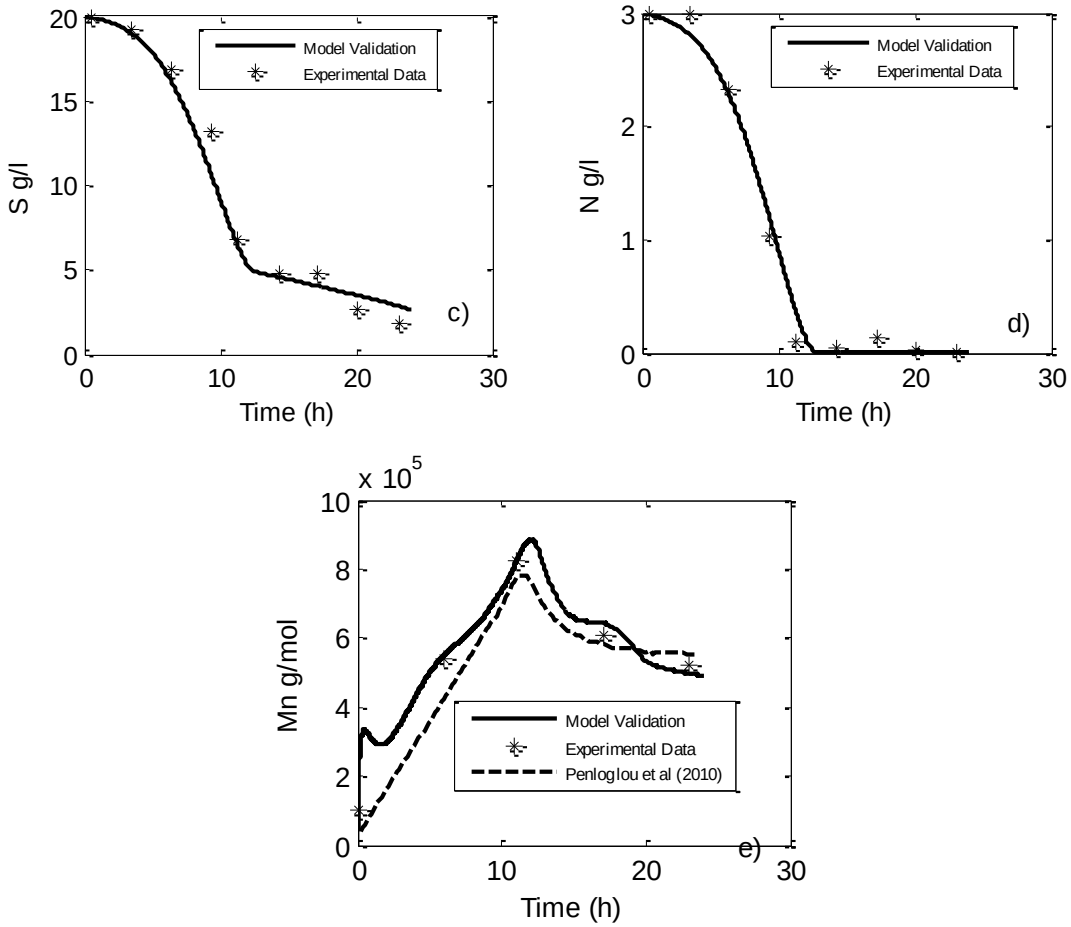

Figure 9 Simulation of different batch Dynamics. a)Biomass, b)Polymer, c) Carbon source, d)Nitrogen Source, e) Number Average Molecular Weight (Mn).

3.4.3. Fed-Batch: Structured kinetic/Polymerization Model

As the optimizing control strategy proposed in this work will be applied to a fed-batch process, it is necessary to validate the kinetic/polymerization model under fed-batch conditions. Figure 16 shows the model validation results, including Mn predictions. As it can be seen, model predictions are still in good agreement with experimental data for the product and substrate concentrations and for the average number molecular weight. Figure 16-e) compares the simulation results obtained in this work by solving the

problem using the fixed pivot technique, against the predictions obtained by [38] and the reported experimental data.

Table 9 shows a comparison between the reported kinetic constants [38], [46] and the identified parameters by optimization. Some differences could be due to the differences in the number of parameters used in each model, but result shows a good fitting with the reported parameters.

Table 9 Parameters of the polymerization–depolymerization model.

Parameters	**Authors Estimation** [38]**,** [46]	**Adjusted Parameters**
k_i (h^{-1})	$0.62 \pm 9 \times 10^{4}$	0.64×10^{4}
k_P(h^{-1})	$0.46 \pm 5 \times 10^{5}$	0.44×10^{5}
k_t^* (h^{-1})	$0.14 \pm 1 \times 10^{1}$	0.101×10^{1}
k_{m1}^*(h^{-1})	$0.11 \pm 2 \times 10^{-3}$	0.114×10^{-3}
k_{m2}(l/mol/h)	$0.85 \pm 15 \times 10^{7}$	0.75×10^{7}
k_d^*(h^{-1})	$0.83 \pm 6 \times 10^{2}$	0.25×10^{2}
$\frac{Y_M}{F}$	$0.35 \pm 2 \times 10^{-2}$	0.23×10^{-2}

After validating the simulation results for the fed-batch kinetic/polymerization model and its interaction with the macroscopic model, it is possible to use such model in order to get enough “in silico data” for building a state estimator able to predict the number average molecular weight, the weight average molecular weight and the polydispersity index.

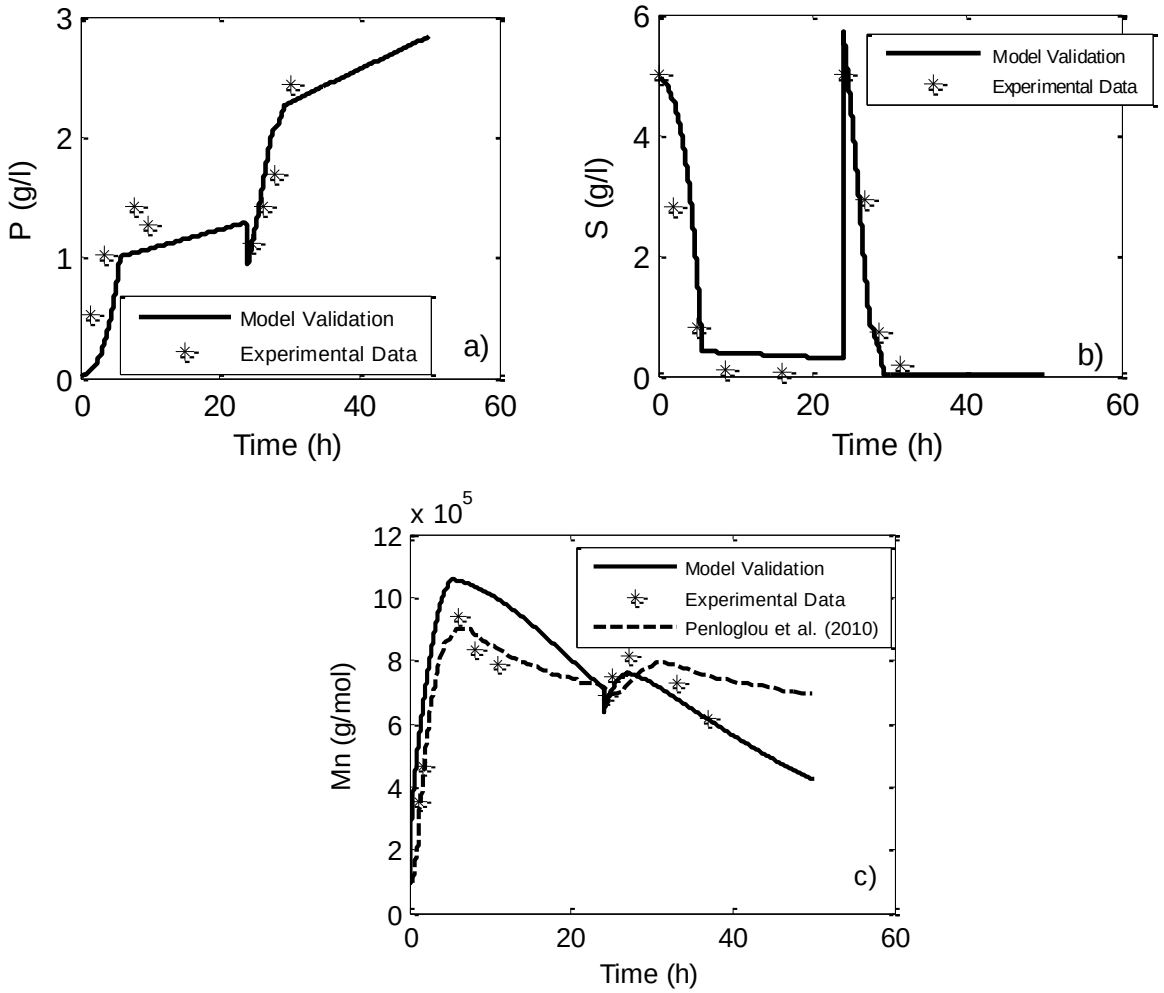

Figure 10 Simulation of different batch Dynamics.a) Polymer, b) Carbon source, c) Number Average Molecular Weight (Mn).

3.5. Soft sensor development for predicting the weight number molecular weight (Mw) and the number average molecular weight (Mn)

An Artificial Neuronal Network (ANN) was developed for being used as state estimator for the present case study. The ANN was developed by using the “in silico” data obtained from the kinetic/polymerization model described in the previous section. The ANN was selected to be used as online estimator instead of the kinetic/polymerization model because the latter has an increased computational demand when used at online

applications. Therefore, towards looking for tools that could be really applied online at industrial level, it was decide to use the ANN for Mw and Mn predictions.

Figure 17 shows the structure of the ANN built. As it can be seen, the ANN is composed by fourteen inputs and one output, twelve neurons in the inner layer and one neuron in the outer layer. The regressor, which is the vector of measured (or known) signals, comprises the following variables [F_1(t-1); F_1(t-2); F_2(t-1); F_2(t-2); X(t-1); X(t-2); S(t-1);S(t-2); N(t-1); N(t-2); P(t-1); P(t-2); CO_2(t-1); CO_2(t-2)]. Two ANNs were built, one for predicting the Mn and the other for predicting the Mw. Therefore, with de predicting Mn and Mw it is possible to estimate PDI.

The “in silico data” for the regressor vector were generated using persistently excited signals, obtained by using random piecewise feeding profiles in a range between 0-10 L/h in the macroscopic model described in sections 3.3 and the kinetic /polymerization model described in section 3.4. In silico data were obtained for building the ANN for Mw prediction, the 70% to those data were used for training and the remaining data were used for validating the ANN. It is important to notice that all the data were normalized between 0-1.

.

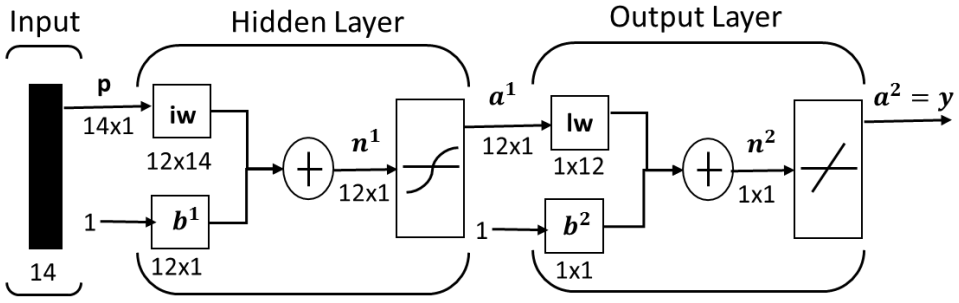

Figure 11 Artificial Neuronal Network built in Matlab 2014b Toolbox

3.5.1 Mn: ANN Training, Identification and Validation

A script code developed by [69] and the Matlab Toolbox “newfft” were used for building a feed-forward back propagation neural network. Neurons in the inner and outer layers use a hyperbolic tangent function (tansig) as activation function. The output neuron use a linear activation function (purelin). The Levenberg-Marquardt backpropagation (using the ‘trainml’) and the Gradient descent with momentum weight and bias (using the ‘learngdm’) methods were used for training and learning functions, respectively. Finally, the MSE was used as performance index.

The results during the learning and training procedures for building the ANN for predicting the Mn are shown in Figure 18. As it can be seen, the results show a very good fit, with small deviation with a Mean Absolute Error of 0.85% and R^2 of 0.999. Figure 18-a) shows the ANN response with the initial deviation without training, 18-b) shows the performance index during the training. Figures 18-c) and 18-d) show the comparison for the ANN predictions for the identification and validation data, respectively. Finally, figures 18-e) and 18-f) show the fitting response and error variation during training. The histogram shows how the error is reduced with time and it corresponds with the fitting.

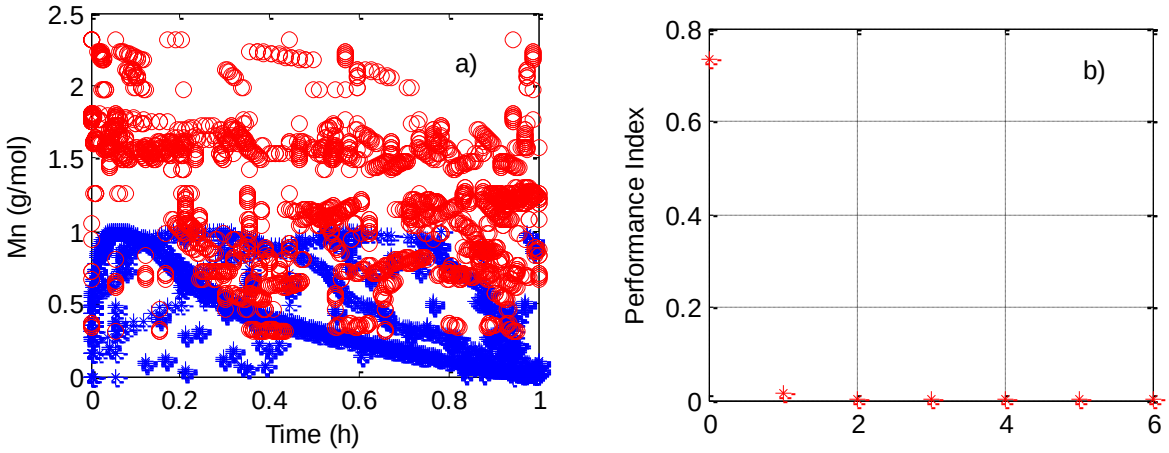

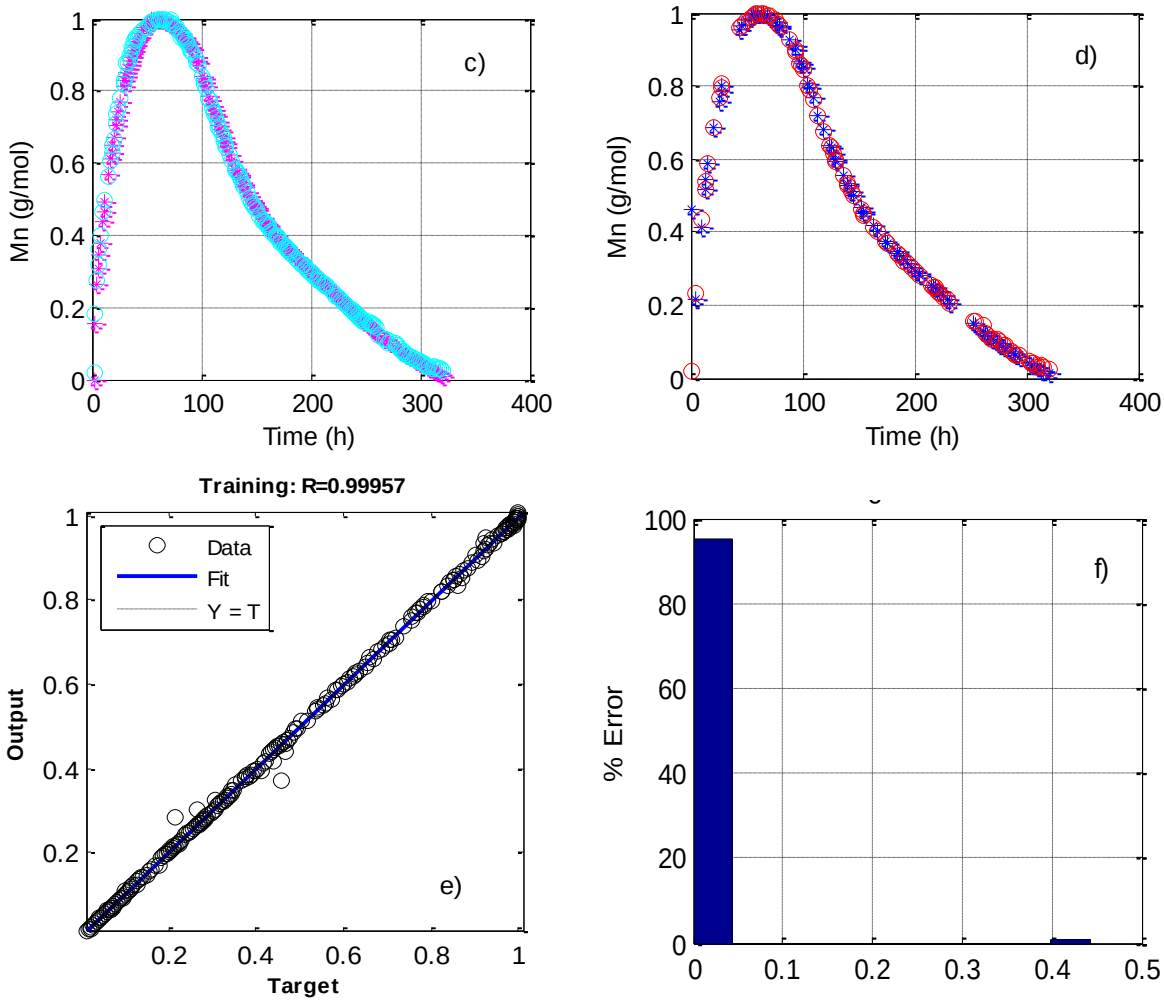

Figure 12 a) Mn ANN response without Learning, ANN prediction (red), Identification Data (blue); b) Performance during Training; c) ANN performance (cyan), Identification Data (Magenta); d) ANN performance (red), Validation Data (blue); e) ANN Training and fitting; f) ANN Histogram with Validation data.

The same methodology was applied for building the ANN for the weight average molecular weight. The results are shown in figure 19. It can be seen that it was found a very good fit with a small deviation with a Mean Absolute Error of 0.78% and R^2 of 0.999.

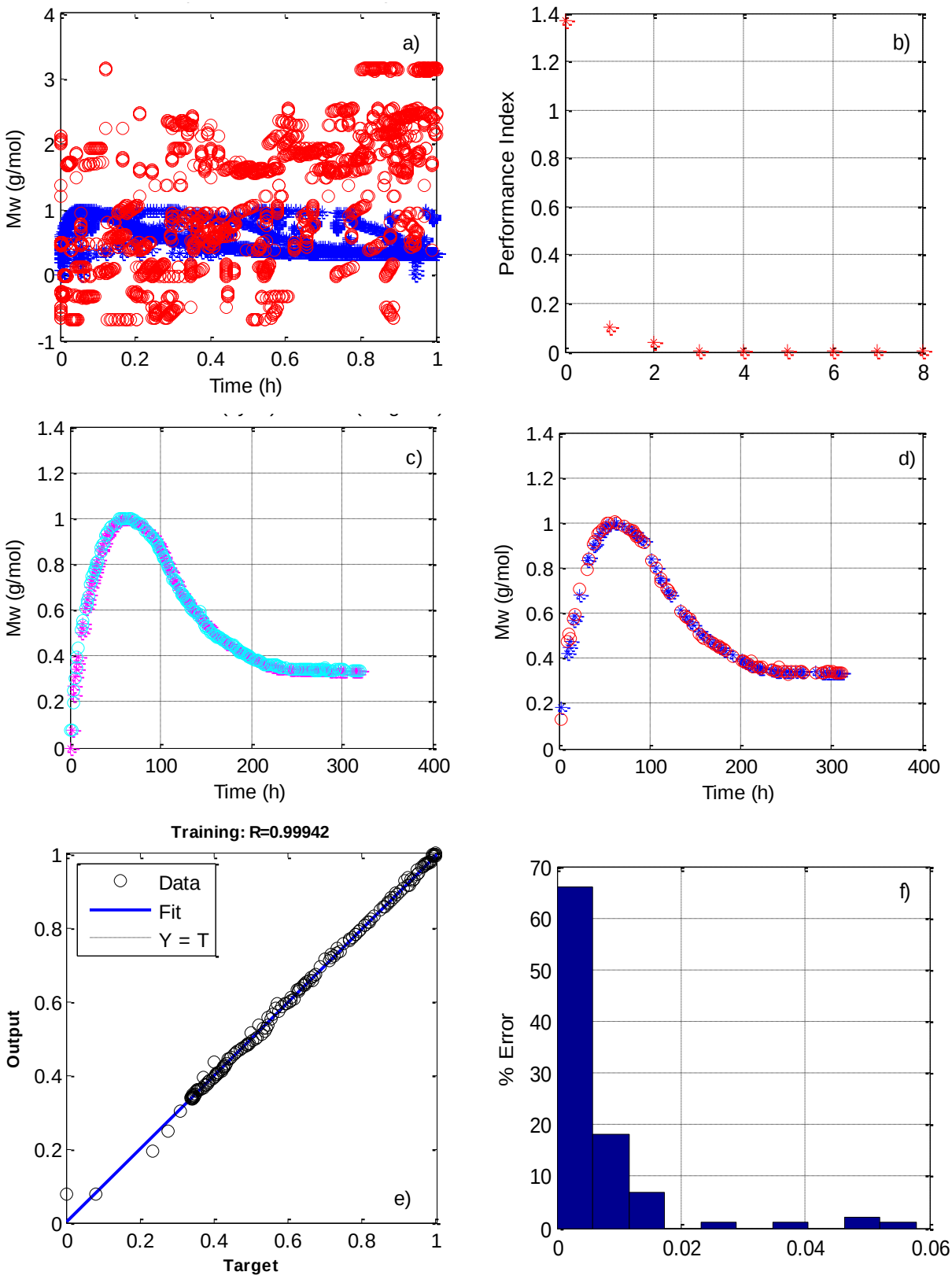
a)
Mw (g/mol)
Time (h)
b)
Performance Index
c)
Mw (g/mol)
Time (h)
d)
Mw (g/mol)
Time (h)
Training: R=0.99942
Data
Fit
Y = T
Output
Target
e)
f)
% Error

Figure 13 a) Mw ANN response without Learning, ANN prediction (red), Identification data (blue); b) Performance During Training; c) ANN performance (cyan), Identification Data (Magenta); d) ANN performance (red), Validation Data (blue); e) ANN training and fitting; f) ANN Histogram with Validation data.

For the weight average molecular weight (Mw), it is important to remind that it is necessary to validate experimentally the model described in section 3-4.

By estimating Mw and Mn it is possible to calculate the polydispersity index. According to [70], the Polydispersity Index (PDI) is a measurement of the dispersion in the polymers. It is defined as the ratio of Mw and Mn. When the polydispersity index is equal to one, then, all the polymeric species in the mass have the same molecular weight and in this case, there not exist dispersion. As higher the index, higher the dispersion in the molecular weight distribution for the polymer. The polydispersity index (PDI) is then calculated as:

$$PDI = M_w/M_n \quad (45)$$

In the next section, the Mn predictions will be used inside an optimizing control strategy in order to allow searching for maximum profitability while keeping end-product properties inside typical desired values. Finally, it will be estimated Mw and PDI in time variations.

4. OPTIMIZING CONTROL

In previous section, it has been established and validated (using reported experimental data) the prediction of state variables and the molecular weight distribution for the fed-batch PHAs fermentation process, using the strain *Ralstonia Eutropha.* In this section, an optimizing control strategy is proposed and applied (in simulation) to the process, in order to maximize the process productivity, while keeping the number average molecular weight between a desired range (i.e. literature reported).

The optimizing control scheme used in this work is given in Figure 20. The optimizing control problem solves a Dynamic Optimization problem (DyOpt), where the decision variables' vector is composed by the manipulated variables (i.e. control vector). For the PHAs fermentation case study, the considered manipulated variables are the feeding profiles for the carbon and nitrogen sources. The DyOpt problem considers a productivity-related objective function, which is subject to constraints (i.e. on the input flows and some state variables). One important point of this optimizing control scheme is that the Mn and Mw are important constraints that should be fulfilled at the optimal solution. The ANN carries out estimation of Mn and Mw

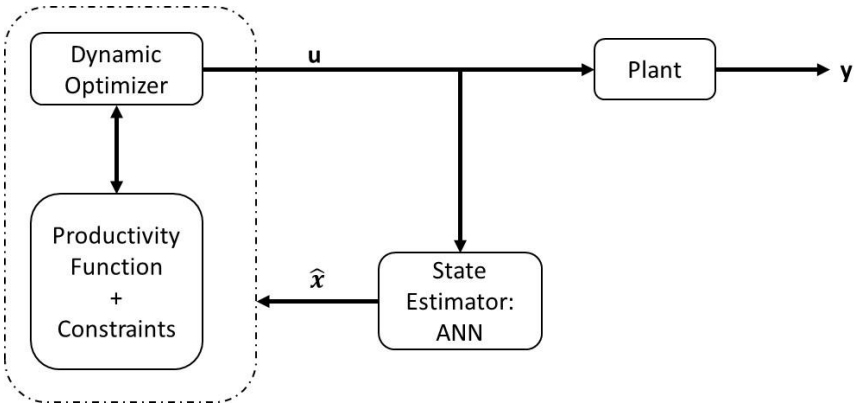

Figure 14 Proposed Optimizing Control Scheme

In the next sections, the optimizing control scheme is applied at two different cases in PHAs fermentation. Case 1 is a reported case study that can be found elsewhere [60]. In

this scenario, the idea is to establish the more suitable feeding strategy in order to assure maximal productivity. For this reason, in this case, four different types of control policies (i.e. feeding strategies) are compared: i) Constant ii) single pulse, iii) piecewise constant, and iv) sinusoidal feeding profiles. On the other hand, Case 2 deals with the optimizing control problem of a PHAs fermentation process using standard conditions, which have been determined by the Biotransformación research group at UdeA. Such standard conditions have been determined in order to avoid inhibition effects in the PHAs fermentation process by R. *Eutropha.* ATCC 17699.

4.1. Case 1: Referenced Case Study: Feeding Policy Selection.

The feeding strategy comparison was based in the fermentation conditions reported in [60], these fermentation conditions are the same reported and validated in [18].

As it was mentioned, the idea is to compare four different feeding policies. The first two strategies (i.e. the constant flow and pulse) are commonly applied due to the easiness on its implementation. The piecewise constant and the sinusoidal policies have been recently reported in the literature.

The sinusoidal feeding policy parameterizes the control vector by using equation (46) in [43], where;

$$u_k = a_{ok} + \sum_{h=1}^{r} a_{hk} Cos\left(w_{hk}\left(\frac{t-t_0}{t_f-t_0}\right) + \emptyset_{hk}\right) \quad (46)$$

In this work, r = 2 in Eq. (46). Therefore, the Carbon and Nitrogen feed flow rate profiles are described by:

$$F_1 = a_{o1} + a_{11} Cos\left(w_{11}\left(\frac{t-t_0}{t_f-t_0}\right) + \emptyset_{11}\right) + a_{21} Cos\left(w_{21}\left(\frac{t-t_0}{t_f-t_0}\right) + \emptyset_{21}\right) \quad (47)$$

$$F_2 = a_{o2} + a_{12}Cos\left(w_{12}\left(\frac{t-t_0}{t_f-t_0}\right) + \emptyset_{12}\right) + a_{22}Cos\left(w_{22}\left(\frac{t-t_0}{t_f-t_0}\right) + \emptyset_{22}\right) \quad (48)$$

Where w_1, w_2 are the frequency, and $\emptyset_1$ and $\emptyset_2$ are the phase angle of the sinusoidal profile. For this specific case, this type of parameterization uses seven parameters for each flow rate.

The piecewise constant feeding strategy is parameterized using equation (49) [71].

$$F_{1,2} = \sum_{j=1}^{m} a_{iok}\varphi(t_{i-1}, t_i)(u_{max} - u_{min}) + u_{min} \quad (49)$$

$$\varphi(t_{i-1}, t_i) = \begin{cases} 0, & t < t_{i-1} \\ 1, & t_{i-1} \leq t < t_i \\ 0, & t \geq t_i \end{cases} \quad (50)$$

Where, for this case were selected m=12 that is the number of steps. u_{max}=0.3 and u_{min}=0 correspond to the maximum and minimum values for each step. The a_{iok} is the parameter that defines the control vector profile, and is therefore the decision variable of the dynamic optimization problem. For this specific case, this type of parameterization uses 12 parameters for each flow rate.

The dynamic optimization problem solved in the optimizing control scheme is described by Equations (51-51h). Bounds for the constraints were taken from the referenced case study described in [60].

$$\underset{F_1(t), F_2(t),\ S_{in}, N_{in}}{Maximize} \ (P(t_f) * V(t_f)) \quad (51)$$

$$\textbf{s.to.}\ F_1 \geq 0\left(\frac{L}{h}\right) \quad (51a)$$

$$0 \leq F_2 \leq 2\left(\frac{L}{h}\right) \quad (51b)$$

$$\max\left(S(t)\right) \leq 90.11\left(\frac{g}{L}\right) \quad (51c)$$

$$\max\left(N(t)\right) \leq 10.11\left(\frac{g}{L}\right) \quad (51d)$$

$$S_{in} \leq 800\left(\frac{g}{L}\right) \quad (51e)$$

$$N_{in} \leq 70\ \left(\frac{g}{L}\right) \quad (51f)$$

$$V \leq 10L \quad (51g)$$

$$\frac{dx}{dt} = f(x, F) \quad (51h)$$

Equation (51) includes constraints on max S and max N, which are the maximum Carbon and Nitrogen source concentration that can be reached in fermentation. In addition, on the S_{in} and N_{in}, which are the Carbon and Nitrogen concentrations in the F_1 and F_2, respectively. Finally, constraints on the values for F_1, F_2 and the volume (V) are also considered.

The dynamic optimization problem was solved by parameterizing the control vector using the four mentioned policies. Figures 21 and 22 show the optimal feeding profiles after solving the problem. As it can be seen, the sinusoidal and piecewise policies have similar profiles. Figures 23 and 24 show the dynamic behavior for the Biomass and Polymer concentrations. It can be seen that the best behavior is obtained when using the sinusoidal feeding profile, followed by the piecewise and constant strategies. The Single pulse strategy resulted in the worst behavior. Figures 25 and 26 show the dynamic behavior for the carbon and nitrogen-source concentrations. The piecewise feeding profile resulted in strong changes in the carbon source concentration. The more suitable behavior is for the sinusoidal and constant feeding strategies, which, resulted in the smoothest response. For the Nitrogen source, both strategies, sinusoidal and piecewise, have the same smoothest profiles.

These tendencies show the importance of feeding strategy selection, according to the type of fermentation, strains, bioreactors and availability of control systems. In the case of high inhibitory fermentations, the selection of the feeding policy, play an important role in order to get a high productivity and profitability, while avoiding cellular stress due to sudden and high variations on the substrate concentration at the culture media. The

sinusoidal feeding strategy is a smooth strategy that can minimize the cellular stress due to big changes in nutrients concentrations.

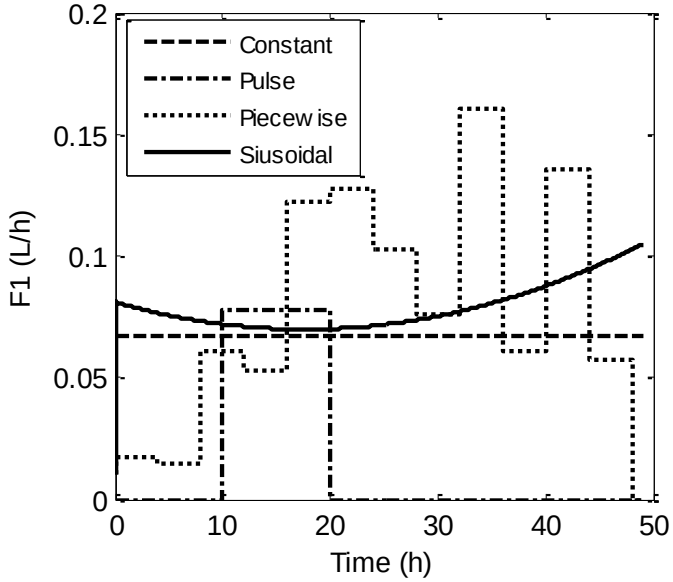

Figure 15 Optimal feeding profiles for the carbon source: Comparison of four policies.

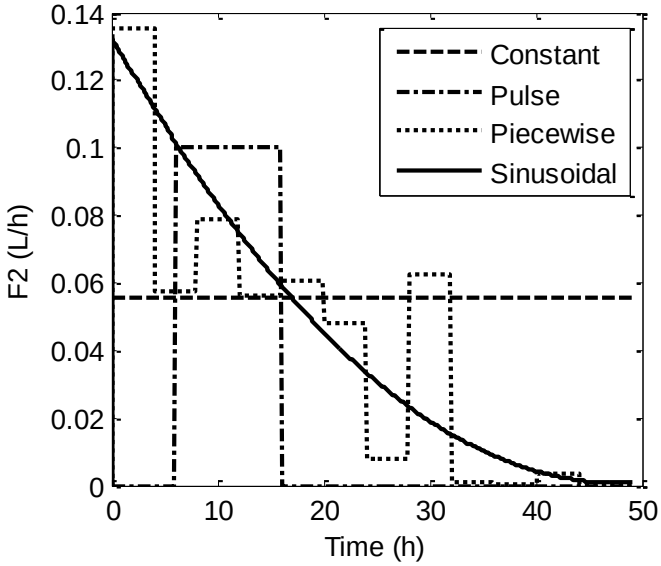

Figure 16 Optimal feeding profiles for the nitrogen source: Comparison of four feeding policies.

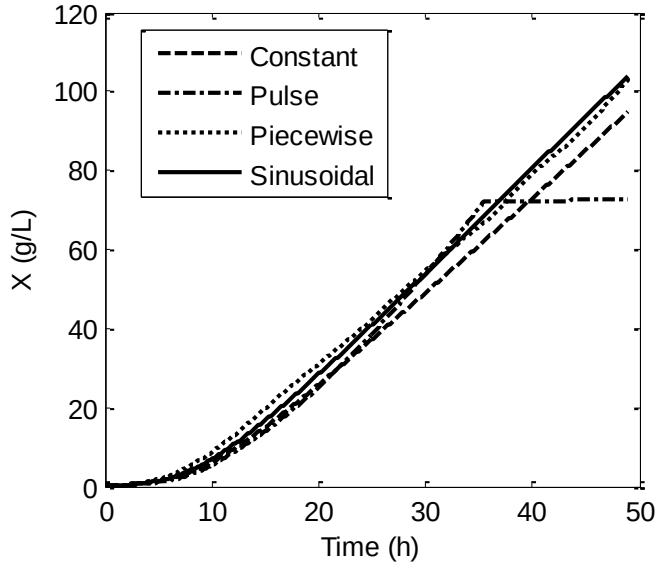

Figure 17 Dynamic behavior of the Biomass: Comparison of four feeding policies.

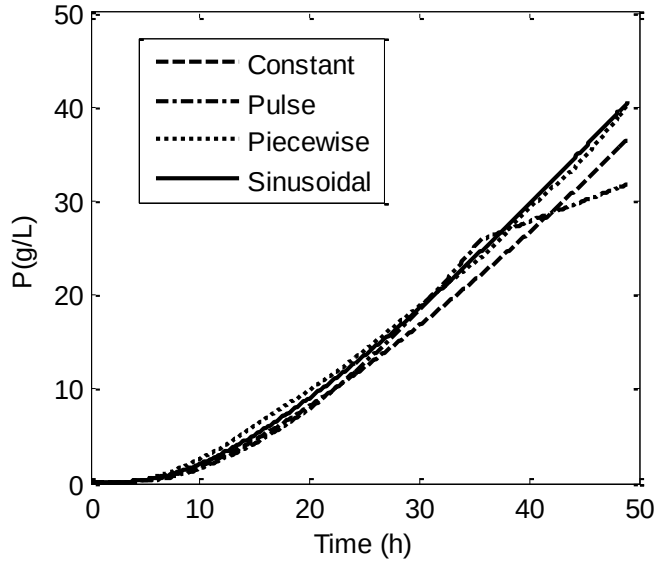

Figure 18 Dynamic behavior of the Polymer concentration: Comparison of four feeding policies.

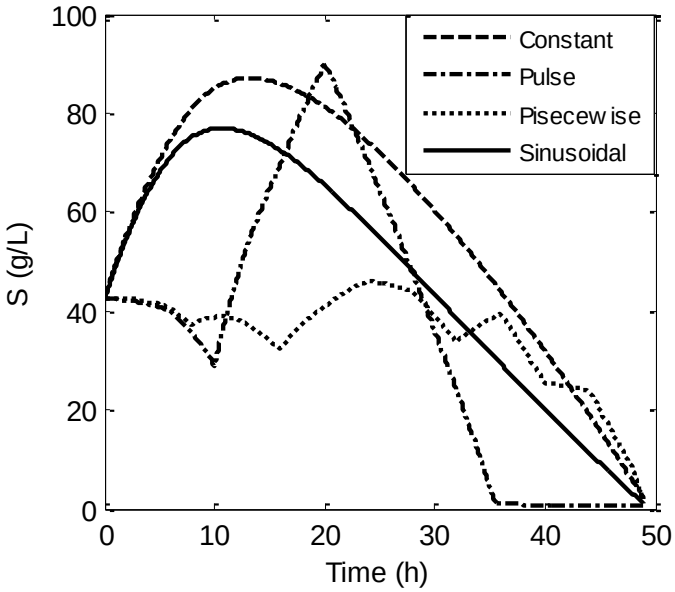

Figure 19 Dynamic behavior of the Carbon source concentration: Comparison of four feeding policies.

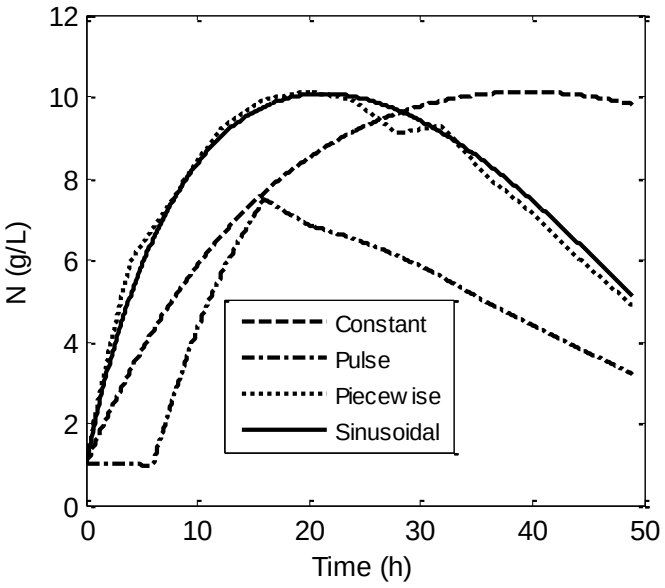

Figure 20 Dynamic behavior of the nitrogen source concentration: Comparison of four feeding policies.

Table 10 compares the results obtained by using the four different strategies. Furthermore, the computational time required for solving the dynamic optimization problem in all cases is also included for the sake of comparison. As it can be seen, the sinusoidal feeding policy resulted in the highest productivity, whereas the single pulse policy resulted in the lowest. Furthermore, the lowest computational time was obtained by the constant and single pulse feeding strategies, whereas the higher one was the one by the piecewise strategy.

The optimal initial substrate and nitrogen-source concentrations are quite similar for all strategies, except for the single pulse (as it was expected), which requires the highest concentration (e.g. 750.59 g/L of carbon source in F_1).

Table 10 Comparison of Feeding strategies: productivity and computational time for the solution of the Dyopt problem for a fermentation time of 49h.

Feeding Strategy	Productivity (g)	Nin (g/L) in F_2	Sin(g/L) in F_1	Computational Time (seconds)
1. Constant	364.45	48.66	495.93	2.87
2. Pulse	183.61	38.44	790.59	2.88
3. Piecewise	402.90	43.37	448.52	4.11
4. Sinusoidal	405.17	42.35	463.61	3.12

Analyzing the results, it is seen that the sinusoidal parameterization is the best strategy due to: i) it reaches the highest productivity by applying a smoother control policy (which avoids cellular stress and possibly substrate shock), and ii) the required computational time for solving the optimization problem is manageable (i.e. in comparison with the piecewise policy it requires a fewer number of parameters to be found during the optimization).

Figures 27-a) and 27-b) show the ANN predictions for Mn and Mw when applying the sinusoidal feeding strategy. Such predictions are compared against the phenomenological-based semiphysical model described in section 3.4. It is important to

remark that the Mw (Figure 27-b) has not been validated against experimental data, but it has a similar behavior as Mn along the fermentation time, and the final values are in the range of the values reported in the literature.

Figure 27-c) show the PDI prediction for sinusoidal feeding strategy based in equation (45). It shows an increase after 30 hours due to the decrease in Mn, while, Mw remains approximately constant.

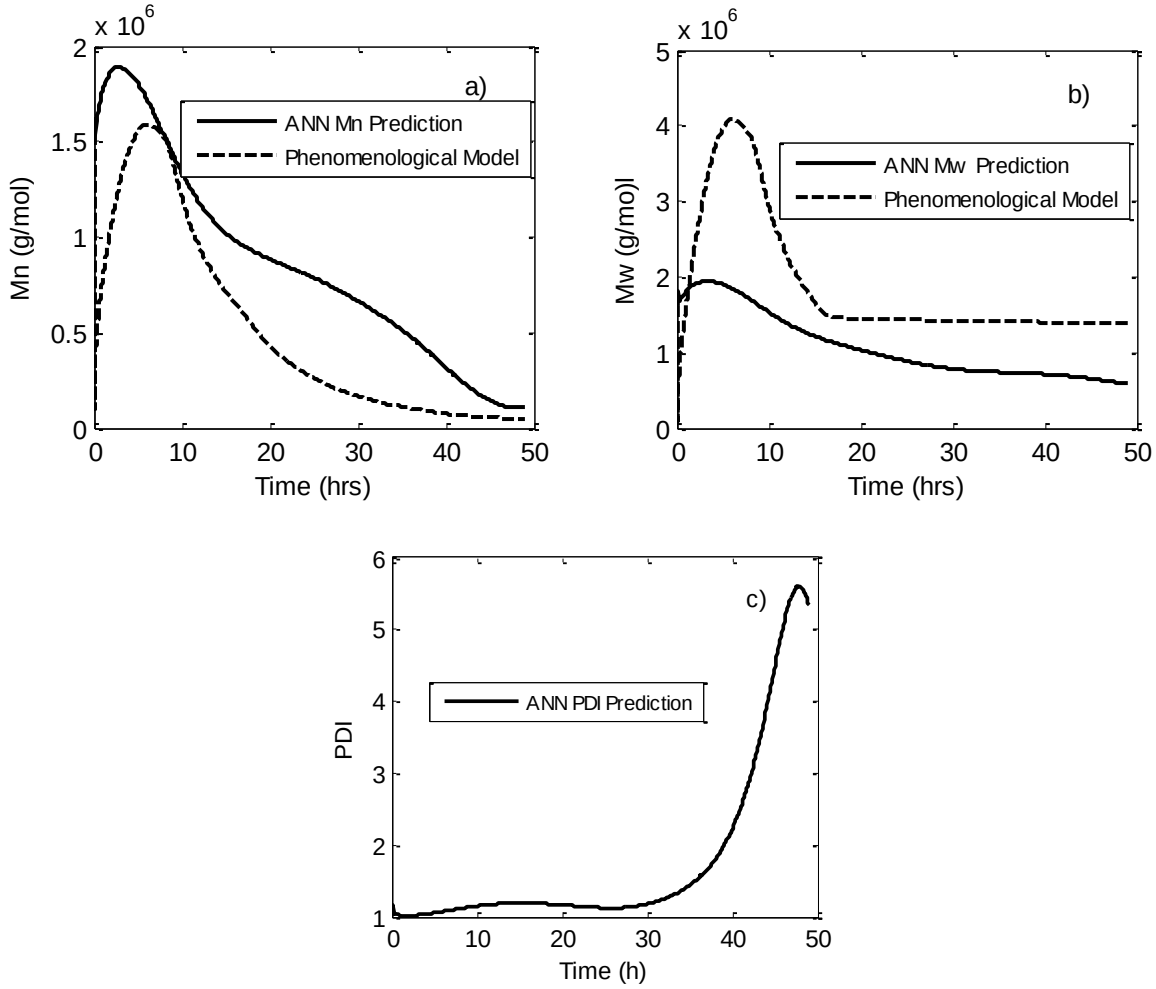

Figure 21 ANN predictions for a) Number Average Molecular Weight distribution (Mn) and b) Weight Average Molecular Weight distribution (Mw). ANN predictions are compared against the phenomenological-based semiphysical kinetic/polymerization model. c) PDI Prediction.

Table 11 shows a comparison between the predictions by the ANN and the phenomenological-based semiphysical kinetic polymerization model developed in section 3.4. The computational time is an important aspect when making this comparison, because application of the optimizing control strategy requires online prediction of the polymer end-properties. As it was expected, the phenomenological-based semiphysical model has the higher computational time, whereas the ANN calculations are faster. However, it is important to notice that more experimental data are required to build a more robust ANN for predicting Mn and Mw. Unfortunately, at this moment to the author´s knowledge, there are on the open literature no more experimental data available than those already used in section 3.4. Finally, it is important to remark that even though ANN predictions differ from those from the phenomenological-based semiphysical model in an order of magnitude, the approximation is good enough and it gives an idea about what is happening with Mn and Mw because ANN predictions are in agreement to the values reported in the literature for the type of fermentation addressed in this work (e.g. fed-batch by *Ralstonia eutropha*), according to [38], the mechanical properties of biopolymers considerably deteriorate when the weight average molecular weight (Mw) is lower than $4x10^5$ Da. Moreover, for thermoplastic applications the value of Mw should be higher than $6x10^5$ Da and typical values of the number average molecular weight (Mn) of PHB, range from $8x10^4$ to $1x10^6$ Da.

Due to the absence of experimental data, at this point, it is not possible to state which model (the ANN vs the semiphysical kinetic/ polymerization) gives the most accurate predictions for the Mn and Mw values. Of course, the semiphysical kinetic/ polymerization model is more reliable because its structure relays on the first principles, although some terms on it are empirical. Also, the model parameters were kept constant at the values determined by using other conditions. On the other hand, the ANN model is a pure black box model that depends strongly on the experimental data used for building and training the network, and as it was mentioned before, in the available literature there is just one report available with Mn data [38], and therefore, more experimental data are required in order to validate the results associated to the Mn and Mw predictions. Although the model predictions are very important and determine the successful implementation of the optimizing control strategy, it is important to emphasize that this work wanted to show the potential application of dynamic optimization

for maximizing the productivity, but coupling some constraints to the optimization problem, specially constrains related to the polymer end-product characteristics.

Table 11 Molecular Weight Predictions for Smooth Feeding: Sinusoidal strategy at the end of the fermentation (49 h).

Prediction Method	Mn (g/mol)	Mw (g/mol)	Computational Time (seconds)
1. Artificial Neuronal Network (ANN)	$1.09x10^5$	$5.83x10^5$	3.12
2. Phenomenological-based semiphysical kinetic/ polymerization	$4.41x10^4$	$1.38x10^6$	121.08

4.2.Case 2: Specific case study, common Fermentation.

In most common cases during fermentation, inhibition is a big problem that influences negatively the process productivity. This inhibition can be due to many causes, as high initial nutrients concentrations, application of an inappropriate feeding strategy, and a wrong determined dissolved oxygen concentration.

The Biotransformación research group from the University of Antioquia has carried out many studies in order to find the optimal initial conditions that maximize the specific growth rate while minimizing the inhibition effect in fermentations for obtaining PHAs by *Ralstonia eutropha*. ATCC 17699, using as raw material glucose syrup. In this section, the optimizing control problem is solved for this specific case study.

Figure 28 shows the experimental results of the effect of the initial concentration of glucose in the specific growth rate. There were evaluated glucose concentration values from 4 to 30 g/l (concentrations higher than 30g/l were evaluated but showed a strong inhibitory effect).

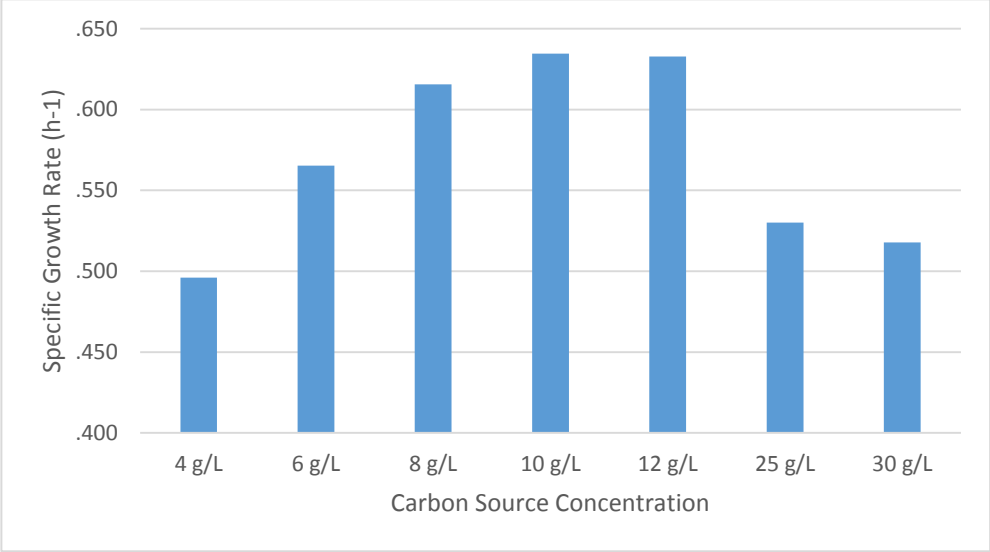

Figure 22 Growth inhibition due Initial carbon source concentration in PHAs production by *Ralstonia eutropha.*

The same analysis was performed for the Nitrogen source (ammonium sulfate in balanced medium), concentrations higher than 10.11 g/l showed an inhibitory effect. The dissolved oxygen concentration is kept at 40% D.O, by having an airflow rate of one Vessel Volume per Minute (VVM). The initial Polymer concentration is almost equal to zero and the initial Biomass concentration is 0.18 g/L. The dynamic optimization problem to be solved is given in equation (52):

$$\underset{F_1(t),\,F_2(t),\;S_{in},\,N_{in}}{Maximize}\ \left(P(t_f) * V(t_f)\right) \tag{52}$$

$$\textbf{s.to. } F_1 \geq 0.3\left(\frac{L}{h}\right) \tag{52a}$$

$$F_2 \leq 0.3\left(\frac{L}{h}\right) \tag{52b}$$

$$\max\left(S(t)\right) \leq 30\ \left(\frac{g}{L}\right) \tag{52c}$$

$$S(t_f) \leq 0.8S(t_0),\ \left(\frac{g}{L}\right) \tag{52d}$$

$$\max\left(N(t)\right) \leq 10.11\left(\frac{g}{L}\right) \tag{52e}$$

$$N(t_f) \leq 0.8N(t_0), \left(\frac{g}{L}\right) \tag{52f}$$

$$S_{in} \leq 800\left(\frac{g}{L}\right) \tag{52g}$$

$$N_{in} \leq 70\ \left(\frac{g}{L}\right) \tag{52h}$$

$$V \leq 7L \tag{52i}$$

$$400000\left(\frac{g}{mol}\right) \leq Mn(t) \leq 2000000\ \left(\frac{g}{mol}\right) \tag{52j}$$

$$\frac{dx}{dt} = f(x, F) \tag{52k}$$

Where the objective function is the productivity quantified as P*V at the final time (32 h), max S and max N are the maximum “desirable” Carbon and nitrogen source concentrations (due to inhibition), $S(t_f)$, $N(t_f)$, are the final Carbon and nitrogen source concentrations, which must be below 80% of the Initial concentrations, in order to avoid inhibition conditions and to increase de Yield of substrate respect to biomass gS/gX. S_{in} and N_{in} are the Carbon and Nitrogen source concentrations in F_1 and F_2 respectively. V is

the final fermentation volumen, Mn is the Number Average Molecular Weight, and it must be kept at a range of $4x10^5$-$2x10^6$ g/mol, which according to [46] is a range for having good thermoplastic applications.

The dynamic optimization problem stated in Equation (52) was solved by using the direct approach and parameterizing the control vector by using the sinusoidal parameterization. In Figures 29-a) and 29-b) the obtained optimal feeding profiles for F_1 and F_2 are shown. Figures 29-c) and 29-d) show the Nitrogen and Carbon source concentration along the fermentation. Figures 29-e) and 29-f) show the Polymer and Biomass predicted profiles. Figure 29-g) and 29-h) show the Mn and Mw predictions. Mn predictions are between the desired ranges (i.e. constraint used for assuring end-product specifications). Finally, Figure 25-i) shows the predictions of the polydispersity index. Results for the polydispersity index are also in agreement with the required values for desired PHAs applications, according to [44].

The variation in PDI after time 20h in Figure 25-i) is due to the time variation in Mn looking to fulfill the constraint and the carbon source variation in Figure 25-d) looking for the optimum. It seems to be that Mn changes in a faster way than Mw does. It is necessary to take into consideration the fact of performing control strategies using and validating Mw and PDI in the Dopt as desired constraints.

It is important to notice, in Figures 25-g) and 25-h), the comparison between the ANN and the phenomenological based model predictions. Both models show a similar tendency in the final behavior, but with a deviation in the initial stage. Mw is the most deviated, and this is due to the absence of validation during the development of the ANN.

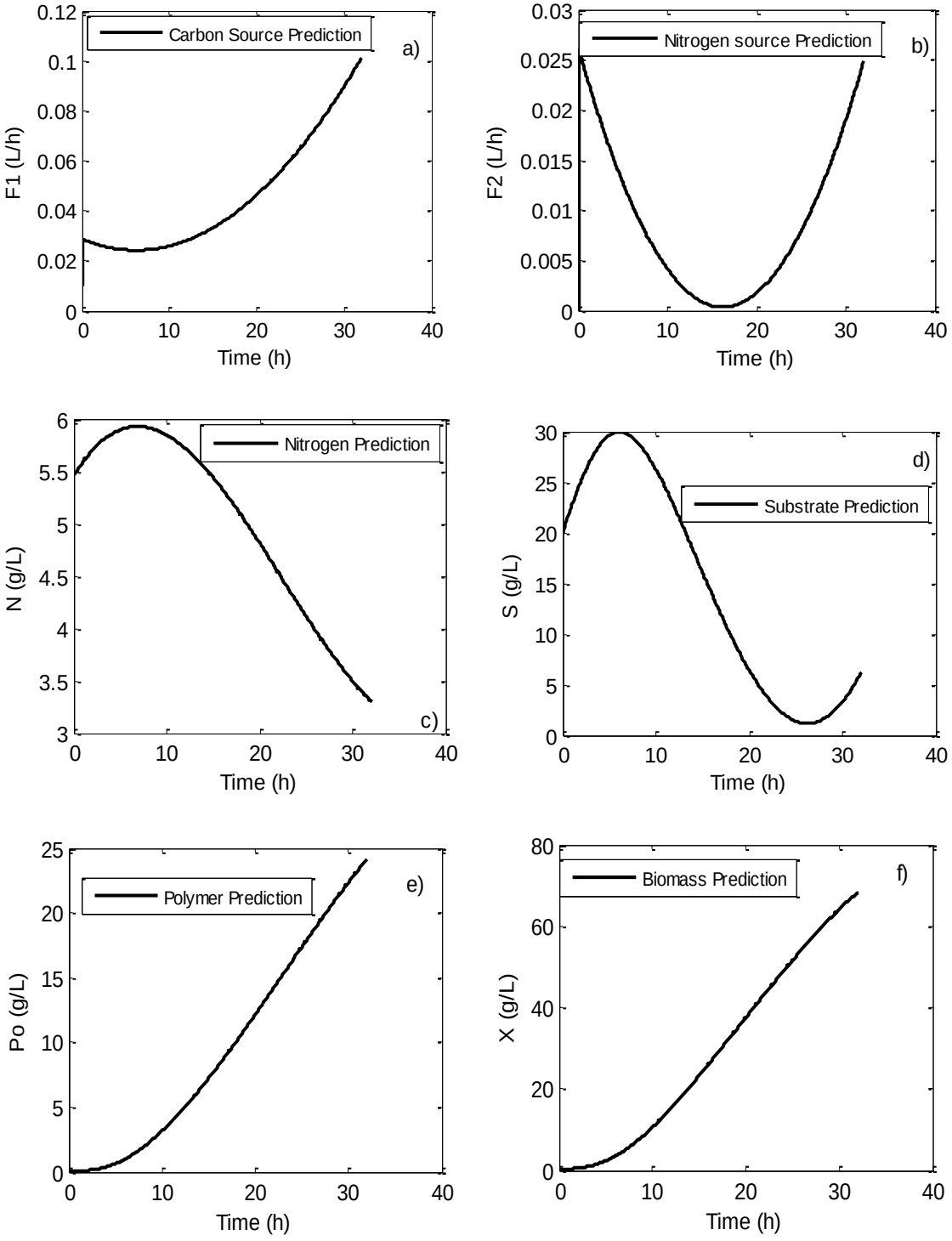
Carbon Source Prediction
a)
F1 (L/h)
Time (h)
Nitrogen source Prediction
b)
F2 (L/h)
Time (h)
Nitrogen Prediction
c)
N (g/L)
Time (h)
Substrate Prediction
d)
S (g/L)
Time (h)
Polymer Prediction
e)
Po (g/L)
Time (h)
Biomass Prediction
f)
X (g/L)
Time (h)

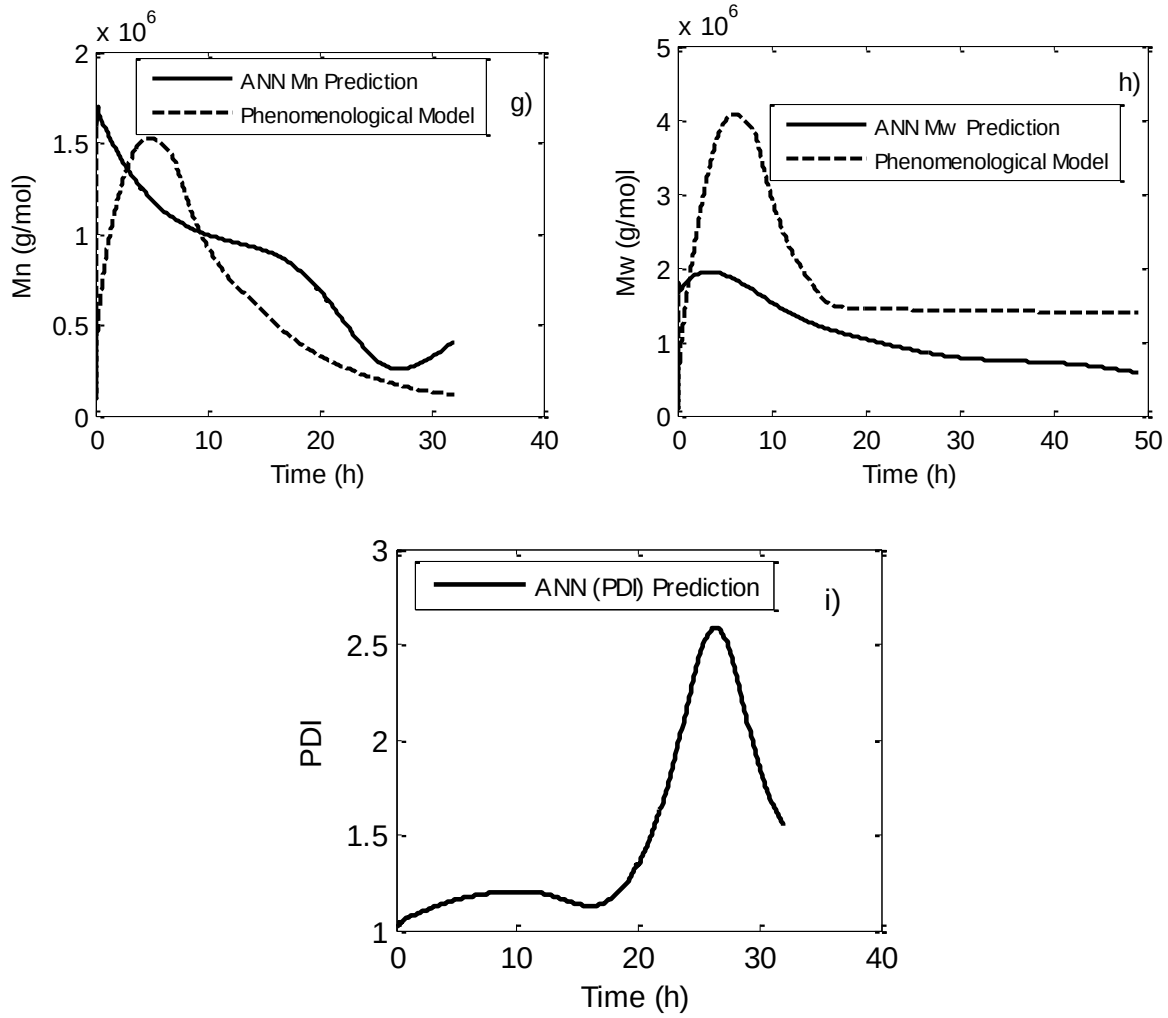

Figure 23 a) Feeding Strategy for Carbon Source. b) Feeding Strategy for Nitrogen Source. c) Nitrogen Source Profile. d) Carbon Source Profile. e) Polymer Profile. f) Biomass Profile. g) Number Average Molecular Weight (Mn); ANN prediction. h) Weight Average Molecular Weight (Mw); ANN prediction. I) Polydispersity Profile.

Table 12 summarizes the obtained results. It can be observed that the final Mn value fulfilled the constraints. Furthermore, it is possible to observe that the productivity reached is 138.44 g, which is a lower value than the obtained in the previous case study, however, conditions worked in the current case study are more realistic. Finally, the final polidispersity is 1.54 that corresponds with literature values for *Ralstonia eutropha* and glucose syrup as raw material [44].

Table 12 Polymer Properties Predictions by ANN at 32h of fermentation.

Prediction Method	**Mn (g/mol)**	**Mw (g/mol)**	**Productivity (g)**	**Polydispersity (PDI)**	**Computational Time (seconds)**
Artificial Neuronal Network (ANN)	$4.05x10^5$	$6.25x10^5$	138.44	1.54	2.34

4.3. Disturbances Scenarios

In this section, the dynamic behavior of the main process variables was analyzed when facing different disturbances scenarios (i.e. variations of ±50% in the nominal value of the most important parameters or process conditions) such as maximum specific growth rate and initial conditions such as biomass and carbon concentrations. Those are the most common disturbances in fermentation processes that affect the final productivity.

The disturbances scenarios are compared to the nominal case (Case 2, Specific case study in section 4.2). Table 12 shows the analyzed scenarios and the final productivity reached due to the variations in the nominal value of the mentioned parameters. The optimizing control problem was solved again at each evaluated scenario, looking for the best feeding policies in order to keep a maximal productivity.

Table 13 Productivity at the final fermentation time evaluated for different disturbances scenarios in 32 h and 7 L.

Parameters		**Productivity (g)**
μ_m	**-50%**	49.49
	Nominal: 0.61 h^{-1}	138.43
	+50%	242.77
$\mathbf{X}_{(t0)}$	**-50%**	143.76
	Nominal: 0.18 g/L	138.43
	+50%	152.38
$\mathbf{S}_{(t0)}$	**-50%**	169.79
	Nominal: 20 g/L	138.43
	+40%	158.85

In Table 13 is possible to see the positive effect in the productivity due to +50% of change in the nominal value of the maximum specific growth rate. This could be due to the effect of increasing the biomass and in this sense the polymer concentration. Figures 30-a) and 30-b) show the optimal feeding policies due to the disturbances in the maximum specific growth rate. Figures 30-c), 30-d), 30-e) and 30-f) show the optimal response due to the change in the feeding polices. If μ_m decreases, the biomass concentration decreases as well, which results in an important reduction on the process productivity (from 138.43 g at the nominal case, to 49.49 g).

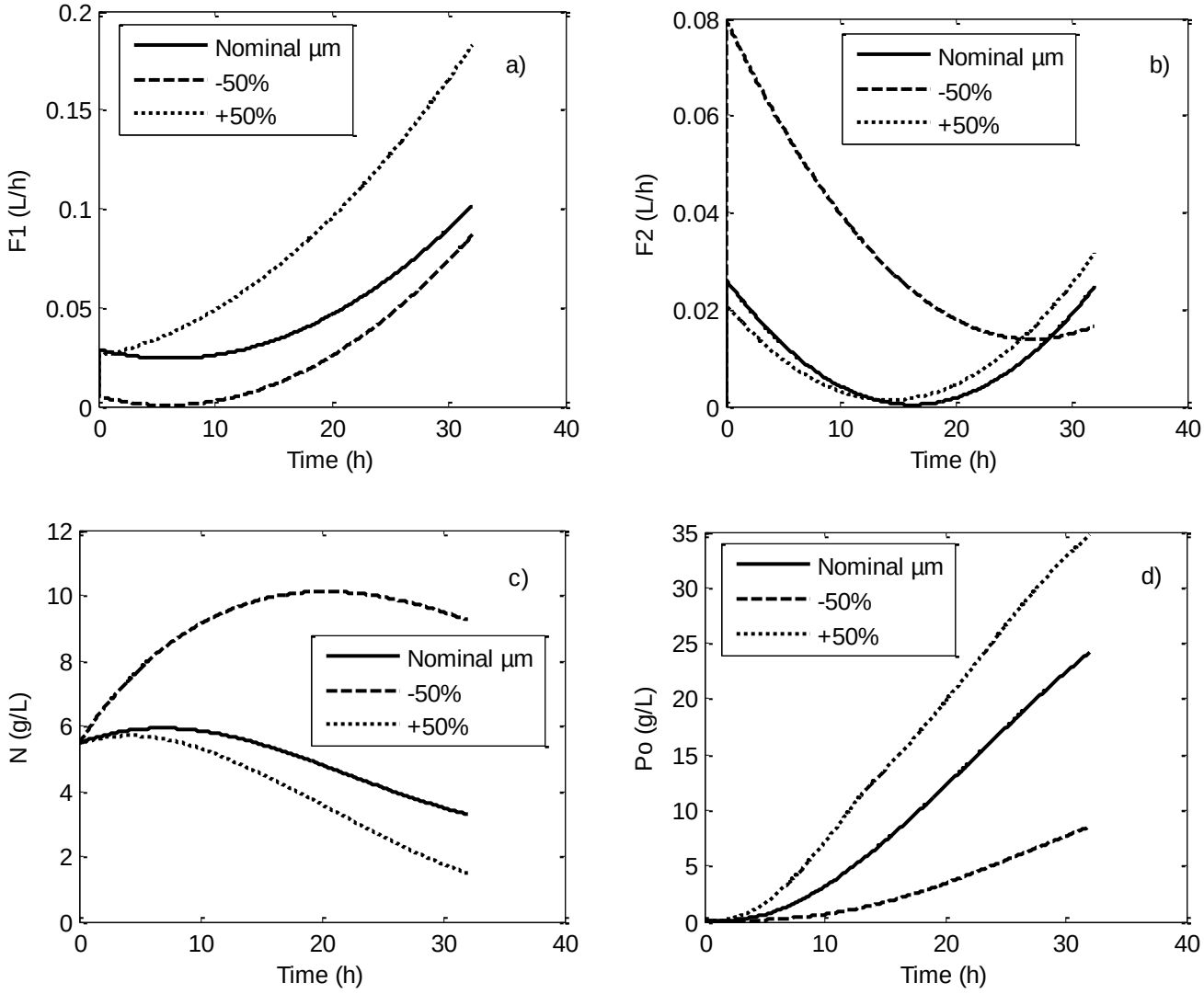

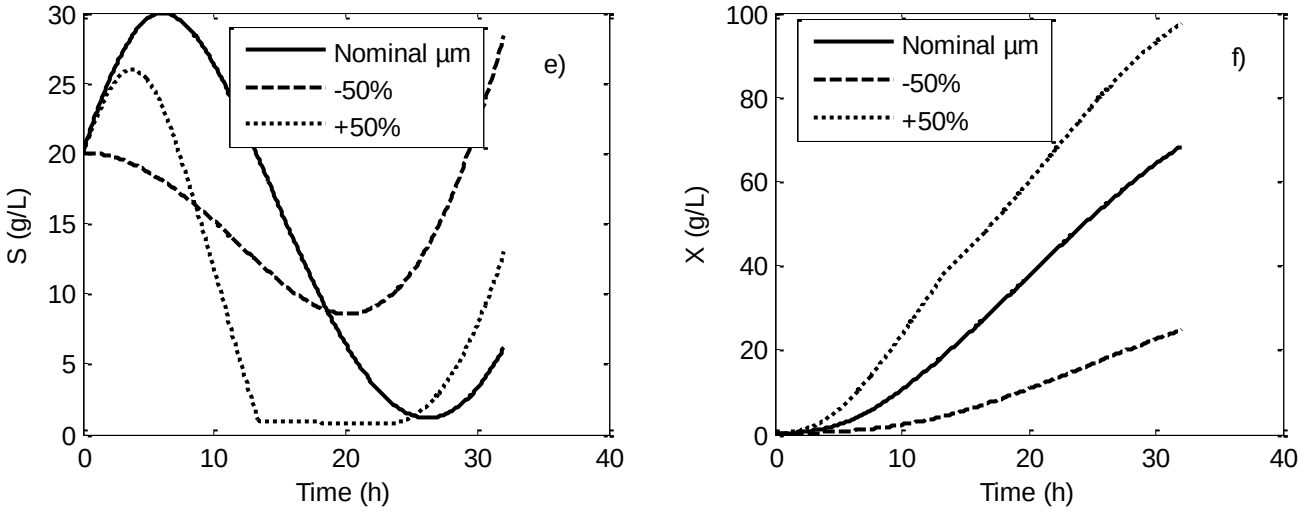

Figure 24 Disturbances due to the change in μ_m a) Carbon Source feeding polices; b) Nitrogen source feeding Polices; c) Nitrogen Source Profile; d) Polymer Profile; e) Carbon Source Profile; f) Biomass Profile.

The same evaluation was performed when varying the initial biomass concentration, whose results can be seen in Figures 31-a) to 31-f). Figures 31-a) and 31-b) show the optimal feeding policies to reach a productivity of 152.38 g with a +50% of change in the nominal value. Figures 31-d), -e) and -f) show a similar tendency in the concentration profiles due the changes in the feeding polices. Figure 31-c) have an important deviation due the changes in nitrogen feeding polices as Figure 31-b) shows.

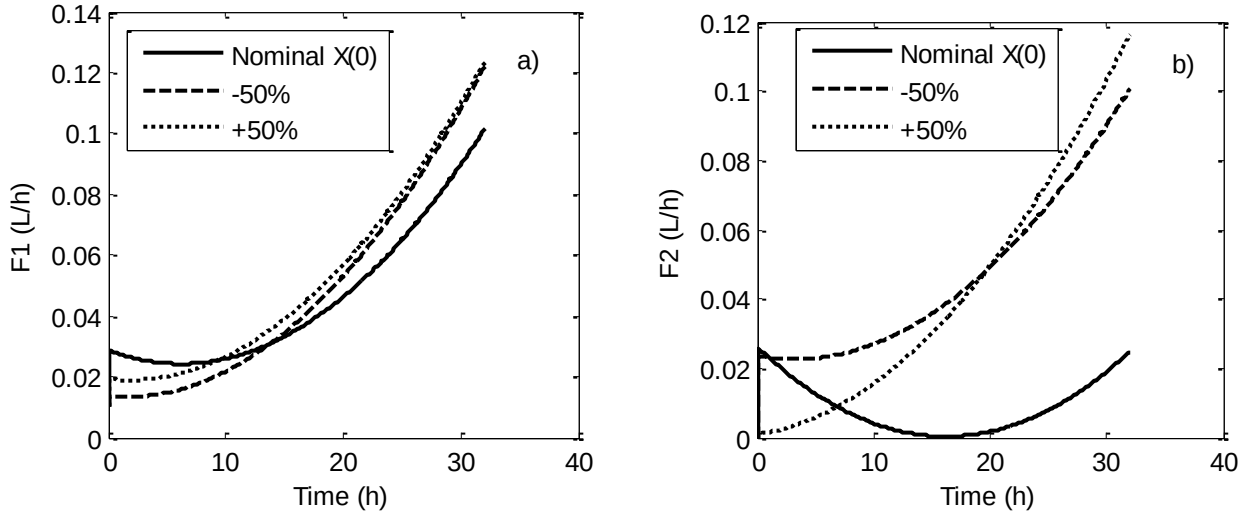

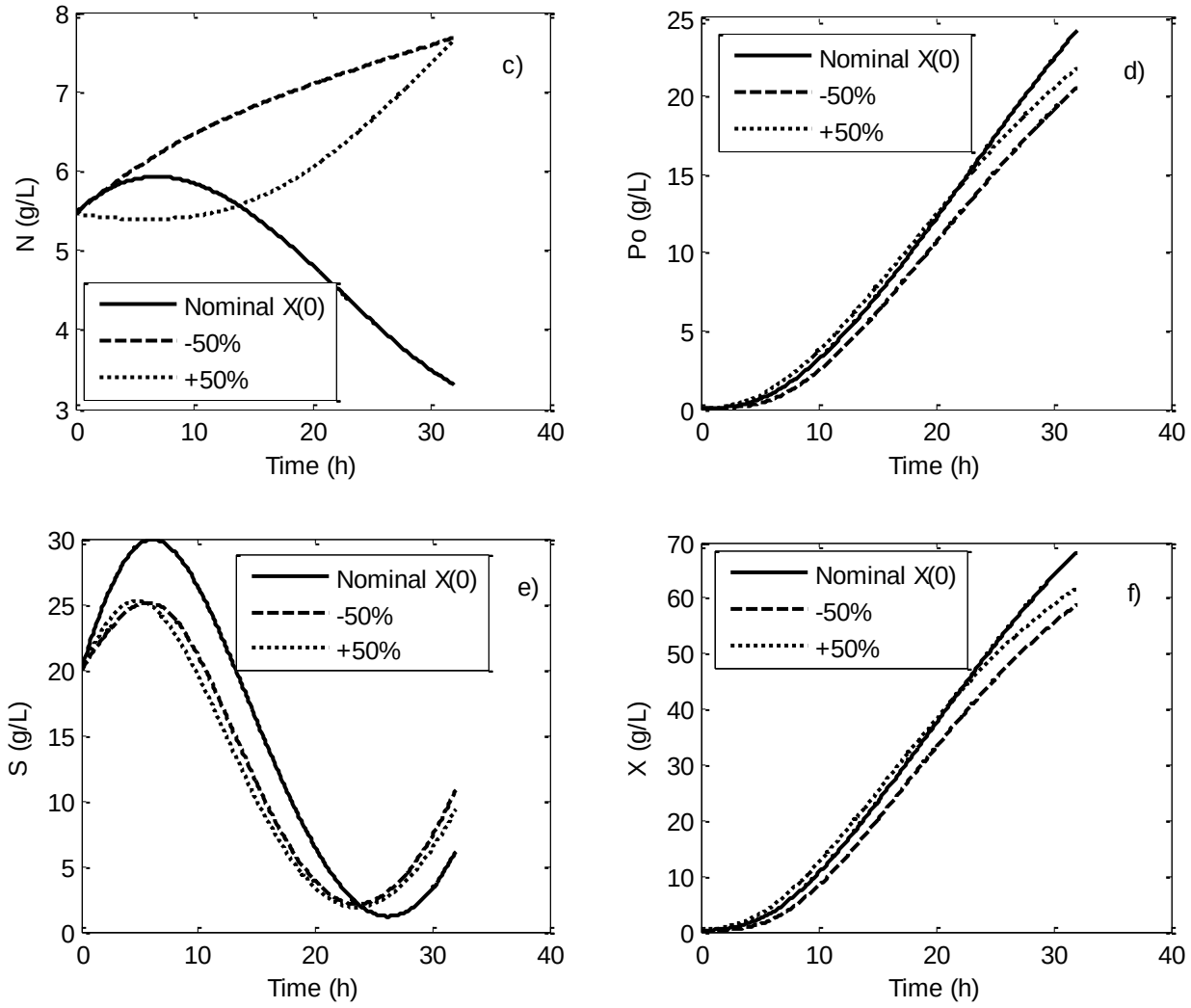

Figure 25 Disturbances due to the change in initial Biomass concentration X(0) a) Carbon Source feeding polices; b) Nitrogen source feeding Polices; c) Nitrogen Source Profile; d) Polymer Profile; e) Carbon Source Profile; f) Biomass Profile.

Figures 32-a) and –b) show the feeding polices due the change in the initial carbon source concentration. It was performed -50% of change in the nominal value of the initial state and +40% of change in the nominal value of the initial state, because of the constraint, in order to avoid inhibition conditions (at concentrations higher than 30 g/L).

Figures 32-d) and –f) shows a similar tendency with respect to the feeding polices changes. Nevertheless, Figures 32-c) and e) show an important deviation from the nominal value due the changes in the concentration profiles.

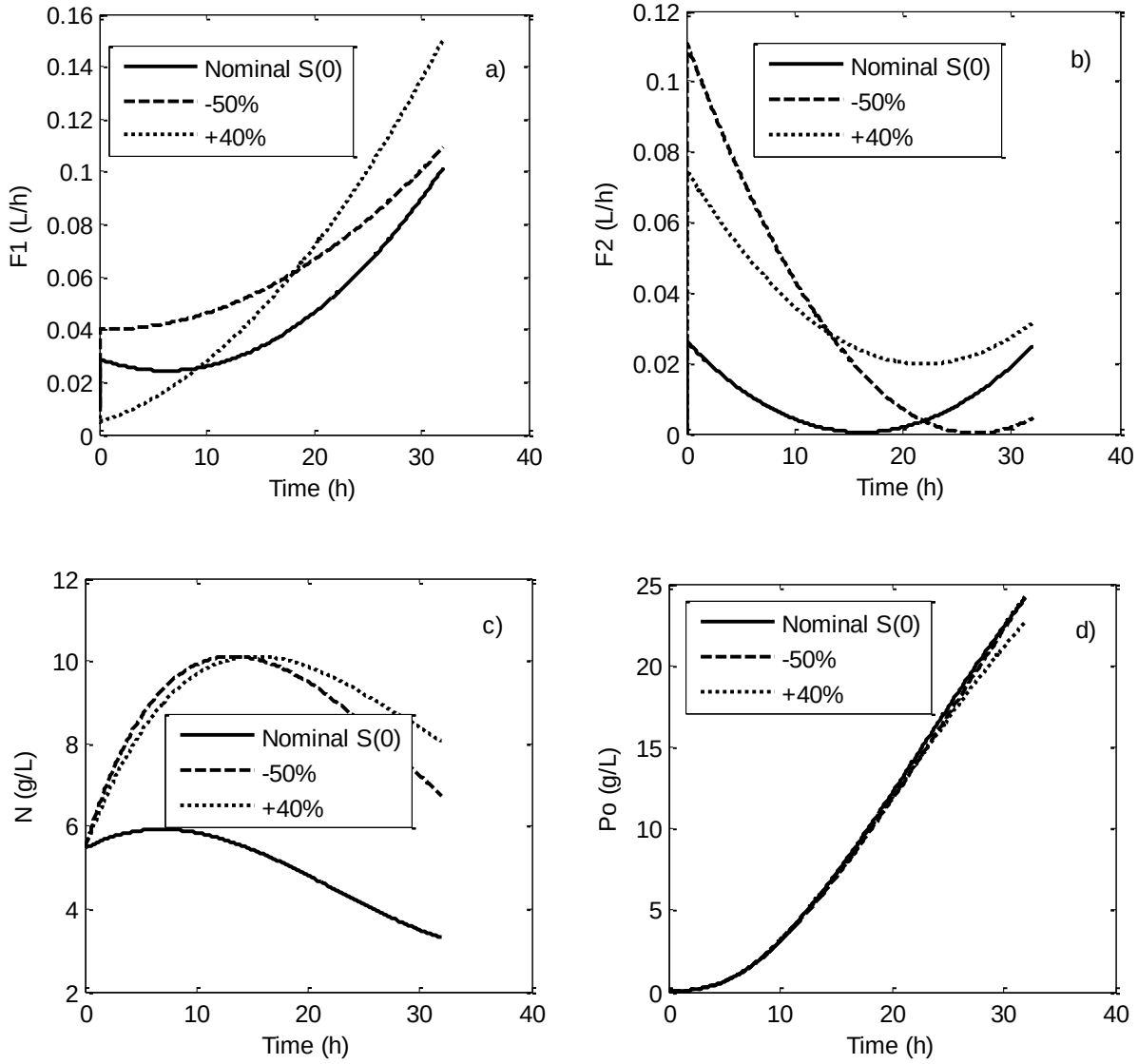

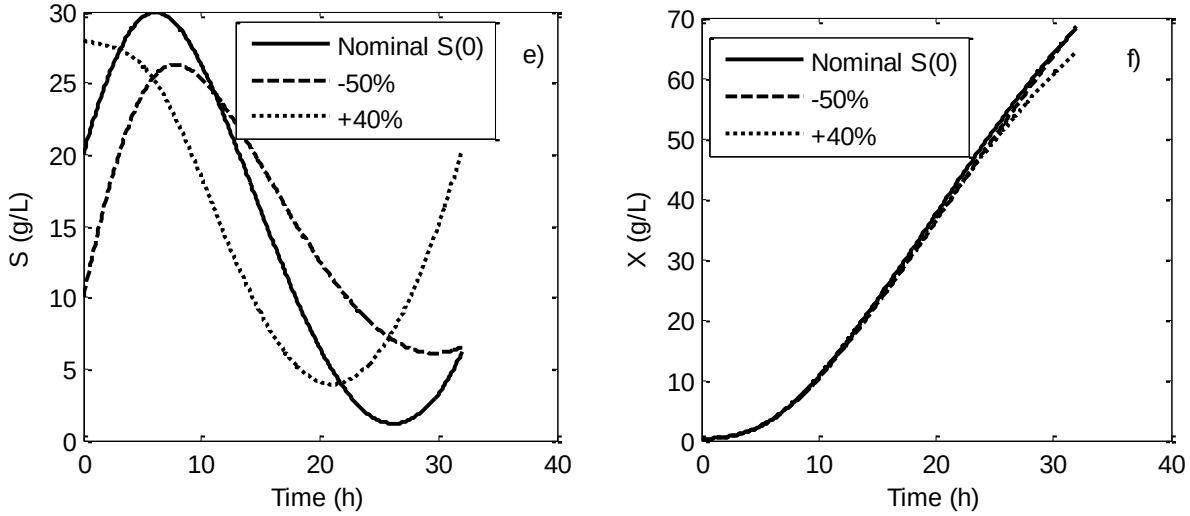

Figure 26 Disturbances due to the change in initial Carbon Source concentration S(0) a) Carbon Source feeding polices; b) Nitrogen source feeding Polices; c) Nitrogen Source Profile; d) Polymer Profile; e) Carbon Source Profile; f) Biomass Profile.

5. CONCLUSIONS

Advanced control strategies, as optimizing control, are essential tools that can be implemented in order to achieve maximal productivity and profitability in bioprocess applications. By applying the optimizing control concept coupled to a soft-sensor for predicting number average molecular weight, it was possible to reach a high productivity while keeping desired end-product specifications.

Sinusoidal parameterization has shown to provide higher productivity through the use of smooth feeding profiles that are suitable for avoiding cellular stress due to substrate shock. Furthermore, as such, parameterization uses a lower number of parameters; the dynamic optimization problem was solved in a faster way, when compared to a traditional piecewise parameterization.

In the disturbances scenario analysis it was possible to observe that when important process parameters change, it is necessary to solve once again the optimizing control problem, in order to look for the best new feeding policies leading to a higher productivity while fulfilling the constraints in the Mn.

For real case applications it is necessary to think about implementation issues, where the minimum requirements will be a computer based control system and final control elements (i.e. proportional valves, variable speed drive pumps).

More experimental data are required for validating the Mw and the PDI in order to obtain more accurate predictions for fulfilling the constraints in the solution of the optimizing control problem.

Further work is now directed towards applying the optimizing control-ANN strategy developed here in a 500L pilot plant located at the Biotransformación research group lab, for producing polyhydroxyalkanoates, by using as raw material a mixture of vinasses/molasses as carbon source.

6. RESEARCH PRODUCTS

- International Symposium BIOFARBICAS, "Model based multi-objective optimization as a tool for Maximizing productivity in bioprocesses: case study polyhydroxyalkanoates production ", Medellin August 2015.

- XI Scientific Technical Conference on Chemical Engineering, “Advanced control of a fed-batch reaction system to increase the productivity in the polyhydroxyalkanoates production process”, University of Cartagena, May 2016.

- CLCA Latin American Conference on Automatic Control, “Advanced control of a fed-batch reaction system to increase the productivity in the polyhydroxyalkanoates production process”, EAFIT University, October 2016.

- Second Chemical Engineer Symposium -Bioprocess Winter School, “Advanced control of a fed-batch reaction system to increase the productivity in the polyhydroxyalkanoates production process”, University of Antioquia, October 2016.

7. REFERENCES

[1] G. Lee and J. Na, "Future of microbial polyesters," *Microbial Cell Factories,* pp. 12-54, 2013.

[2] D. Dietrich, B. Illman and C. Crooks, "Differential sensitivity of polyhydroxyalkanoate producing bacteria to fermentation inhibitors and comparison of polyhydroxybutyrate production from Burkholderia cepacia and Pseudomonas pseudoflava," *BMC Research Notes,* pp. 6-219, 2013.

[3] S. Chanprateep , K. Kikuya , H. Shimizu and S. Shioya , "Model predictive controller for biodegradable polyhydroxyalkanoate production in fed-batch culture," *J Biotechnol,* vol. 2, no. 95, pp. 69-157, 2002.

[4] D. Dochain, "Bioprocess Control," in *Control Systems, Robotics and Manufacturing Series*, United States, WILEY, 2001, pp. 79-111.

[5] C. Cimander, T. Bachinger and C. F. Mandenius, "Integration of distributed multi-analyzer monitoring and control in bioprocessing based on a real-time expert system," *Journal of Biotechnology,* vol. 103, no. 3, p. 237–248, 2003.

[6] J. P. Steyer, P. Buffière, D. Rolland and R. Moletta, "Advanced control of anaerobic digestion processes through disturbances monitoring," *Water Research,* vol. 33, no. 9, p. 2059–2068, 1999.

[7] C. Du, . J. Sabirova, W. Soetaert and C. L. Ki , "Polyhydroxyalkanoates production from low-cost sustainable raw materials," *Current Chemical Biology,* vol. 1, no. 6, pp. 14-25, 2012.

[8] M. Anjali, C. Sukumar, A. Kanakalakshmi and K. Shanthi, "Enhancement of growth and production of polyhydroxyalkanoates by Bacillus subtilis from agro-industrial waste as carbon substrates," *Composite Interfaces,* vol. 2, no. 21, pp. 111-119., 2014.

[9] W. Wu, S. Y. Lai, M. F. Jang and . Y. . S. Chou, "Optimal adaptive control schemes for PHB production in fed-batch fermentation of< i> Ralstonia eutropha," *Journal of Process Control,* vol. 8, no. 23, pp. 1159-1168, 2013.

[10] . M. Titz, K. H. Kettl, K. Shahzad, . M. Koller, . H. Schnitzer and M. Narodoslawsky, "Process optimization for efficient biomediated PHA production from animal-based waste streams.," *Clean technologies and environmental policy,* vol. 3, no. 14, pp. 495-503., 2012.

[11] R. Amache, A. Sukan, M. Safari, I. Roy and T. Keshavarz, "Advances in PHAs Production.," *Chemical engineering transactions,* vol. 32, pp. 931-936, 2013.

[12] A. D. Tripathi, A. Yadav, A. Jha and S. K. Srivastava, "Utilizing of sugar refinery waste (cane molasses) for production of bio-plastic under submerged fermentation process," *Journal of Polymers and the Environment,* vol. 2, no. 20, pp. 446-453, 2012.

[13] S. Kulpreecha , A. Boonruangthavorn , B. Meksiriporn and N. Thongchul , "Inexpensive fed-batch cultivation for high poly (3-hydroxybutyrate) production by a new isolate of Bacillus megaterium," *Journal of bioscience and bioengineering,* vol. 107, pp. 240-245., 2009.

[14] . S. Yi, P. Chih, . W. Wu, M. Janga and Y. Choua, "Biopolymer production in a fed-batch reactor using optimal feeding strategies," *SCI Research Article,* vol. 88, p. 2054–2061, 2013.

[15] P. Bogaerts and V. Wouwerb, "Software sensors for bioprocesses," *ISA Transactions,* vol. 42, p. 547–558, 2003.

[16] J. M. Dias, L. . S. Serafim, P. . C. Lemos, M. . A. Reis and R. Oliveira, "Mathematical Modelling of a Mixed Culture Cultivation Process for the Production of Polyhydroxybutyrate," *Biotechnology and bioengineering,* vol. 9, no. 2, pp. 209-222, 2005.

[17] C. Chatzidoukasa, G. Penlogloub and C. Kiparissides, "Development of a structured dynamic model for the production of polyhydroxybutyrate (PHB) in Azohydromonas lata cultures," *Biochemical Engineering Journal,* vol. 71, p. 72– 80, 2013.

[18] S. Khanna and A. K. Srivastava, "Optimization of nutrient feed concentration and addition time for production of poly(-hydroxybutyrate," *Enzyme and Microbial Technology 39,* vol. 39, p. 1145–1151, 2006.

[19] L. e. a. Lan , "Optimization of polyhydroxyalkanoates fermentations with on-line capacitance measurement," *Bioresource Technology,* vol. 156, p. 216–221, 2014.

[20] S. Suraj and T. Sanjeev , "Soft-sensor development for biochemical systems using genetic programming," *Biochemical Engineering Journal,* vol. 85, p. 89–100, 2014.

[21] A. De Almeida , J. A. Ruiz and N. I. López, "Bioplásticos: una alternativa ecológica," *Química Viva,* 2004.

[22] D. Segura, R. Noguez and G. Espín, "Contaminación ambiental y bacterias productoras de plásticos biodegradables.[Online]," 2010. [Online]. Available: http://www.ibt.unam.mx/computo/pdfs/libro_25_aniv/capitulo_31.pdf. [Accessed 26 Marzo 2011].

[23] K. Sudesh, . H. Abe and Y. Doi, "Synthesis, structure and properties of polyhydroxyalkanoates: Biological polyesters," *Progress in Polymer Science,* vol. 25, pp. 1503-1555, 2000.

[24] R. Chavata, D. Danay and N. Galego, "Miscibilidad de Mezclas Poliméricas de Polihidroxialcanoatos," *Revista Iberoamericana de Polímeros,* vol. 5, no. 2, 2004.

[25] S. SalehMohseni, V. Babaeipour and A. RezaVali, "Design of sliding mode controller for the optimal control of fed-batch cultivation of recombinant E. coli," *Chemical Engineering Science,* vol. 64, pp. 4433-4441, (2009).

[26] S. Nuñez , H. De Battista , F. Garelli , A. Vignoni and J. Picó, "Second-order sliding mode observer for multiple kinetic rates estimation in bioprocesses," *Control Engineering Practice,* vol. 21, p. 1259–1265, (2013).

[27] J. Gonzalez , G. Fernandez , R. Aguilar , M. Barron and . J. Alvarez-Ramirez, "Sliding mode observer-based control for a class of bioreactors," *Chemical Engineering Journal ,* vol. 83 , p. 25–32, (2001) .

[28] H. De Battista , J. Picó and F. Gare, "Specific growth rate estimation in (fed-)batch bioreactors using second-order sliding observers," *Journal of Process Control ,* vol. 21 , p. 1049– 1055, (2011).

[29] P. G. Georgieva and S. F. De azevedo, "Robust control design of an activated sludge process," *Int. J. Robust Nonlinear Control ,* vol. 9, pp. 949-967, (1999).

[30] F. Koumboulis, N. Kouvakas, R. King and A. Stathaki, "Two-stage robust control of substrate concentration for an activated sludge process," *ISA Transactions ,* vol. 47 , p. 267–278, (2008) .

[31] C. G. Schmit , K. Jahan, K. H. Schmit, F. I. Aydinol, E. Debik and V. Pattarkine, "Activated Sludge and Other Aerobic Suspended Culture Processes," *Journal Water,* vol. 3, pp. 806-818, 2011.

[32] G. Goffaux and A. Vande Wouwer, "Bioprocess State Estimation: Some Classical and Less Classical Approaches," *Control and Observer Design,* p. 111–128, 2005..

[33] T. Kichise, T. Fukui, Y. Yoshida and Y. Doi, "Biosynthesis of polyhydroxyalkanoates (PHA) by recombinant Ralstonia eutropha and effects of PHA synthase activity on in vivo PHA biosynthesis," *International Journal of Biological Macromolecules,* vol. 25, p. 69–77., 1999.

[34] . M. Islam , L. Goormachtigh , L. Garcia , H. De Wever and . E. Volckeb, "Modeling pure culture heterotrophic production of polyhydroxybutyrate (PHB).," *Bioresource Technology,* vol. 155, p. 272–280, 2014.

[35] C. A. Riascos and J. M. Pinto, "Optimal control of bioreactors: a simultaneous approach for complex systems," *Chemical Engineering Journal,* vol. 99, p. 23–34, 2004.

[36] D. J. Luvizetto Faccin, I. Martins, N. S. Medeiros Cardozo, R. Rech, M. A. Záchia Ayub, T. L. Moitinho Alves, R. Gambetta and A. Resende Secchi, "Optimization of C : N ratio and minimal initial carbon source for poly(3-hydroxybutyrate) production by Bacillus megaterium," *Journal of Chemical Technology and Biotechnology,* vol. 84, p. 1756–1761, 2009.

[37] M. Tabassum and et al., "Turning waste to wealthbiodegradable plastics polyhydroxyalkanoates from palm oil mill effluent e a Malaysian perspective.," *Journal of Cleaner Production,* vol. 18, pp. 1393-1402, 2010.

[38] G. Penloglou, A. Roussos, C. Chatzidoukas and C. Kiparissides, "A combined metabolic/polymerization:kinetic model on the microbial production of poly(3-hydroxybutyrate)," *New Biotechnology,* vol. 27, no. 4, pp. 1-10, 2010.

[39] G. Penlogloua , E. Kretzaa , C. Chatzidoukasa , S. Paroutib and C. Kiparissidesa, "On the control of molecular weight distribution of polyhydroxybutyrate in Azohydromonas lata cultures.," *Biochemical Engineering Journal,* vol. 62, pp. 39-47, 2012.

[40] A. Nath, M. Dixit, A. Bandiya, S. Chavda and . A. J. Desai, "Enhanced PHB production and scale up studies using cheese whey in fed batch culture of< i> Methylobacterium sp. ZP24," *Bioresource technology,* vol. 13, no. 99, pp. 5749-5755, 2008.

[41] A. N. Amicarelli, O. L. Quintero, F. A. di Sciascio and H. D. Álvarez, "Estudio Comparativo de técnicas para estimación de biomasa en bioproceso tipo batch," in *XXIº Congreso Argentino de Control Automático*, Buenos Aires-Argentina, 2008.

[42] R. Gambetta, "Análise Teórica e Experimental da Curva de Distribuição de Massas Molares do Poli((R)-3-hidróxi-butirato) Produzido pela Bactéria Alcaligenes latus," D.Sc. Thesis, PEQ-COPE/UFRJ, 2006.

[43] S. Ochoa, "A new approach for finding smooth optimal feeding profiles in fed-batch fermentations," *Biochemical Engineering Journal ,* vol. 105 , p. 177–188, 2016.

[44] Y. González García, J. C. Meza contreras, O. González Reynoso and J. A. Córdova López, "Síntesis y biodegradación de polihidroxialcanoatos: plásticos de origen microbiano," *Rev. Int. Contam. Ambie,* vol. 29, no. 1, pp. 77-115, 2013.

[45] F. Morgan-Sagastume, F. Valentino, M. Hjort, D. Cirne, L. Karabegovic, F. Gerardin and A. Werker, "Polyhydroxyalkanoate (PHA) production from sludge and municipal wastewater treatment. Water," *Science & Technology,* vol. 1, no. 69, pp. 177-184., 2014.

[46] G. Penloglou, C. Chatzidoukas and C. Kiparissides, "Microbial production of polyhydroxybutyrate with tailor-made properties: an integrated modelling approach and experimental validation.," *Biotechnology advances,* vol. 1, no. 30, pp. 329-337., 2012.

[47] N. M. Thomson, A. Hiroe, T. Tsuge, D. K. Summers and E. Sivaniah, "Efficient molecular weight control of bacterially synthesized polyesters by alcohol supplementation," *Journal of Chemical Technology & Biotechnology,* vol. 89, p.

1110–1114, 2014.

[48] R. D. Ashby, D. . K. Solaimana, G. D. Strahan and A. C. Levine, "Methanol-induced chain termination in poly(3-hydroxybutyrate) biopolymers: Molecular weight control," *International Journal of Biological Macromolecules,* vol. 74, p. 195–201, 2015.

[49] G. Q. Chen, "A microbial polyhydroxyalkanoates (PHA) based bio- and materials industry," *Chemical Society Reviews,* vol. 38, p. 2434–2446, 2009.

[50] J. P. Gauthier, H. Hammouri and S. Othman, "A simple observer for nonlinear systems: Applications to Biorreactors.," *IEE Transactions On Automatic Control,* vol. 37, no. 6, pp. 875-880, 1992.

[51] J. M. Ali, N. H. Hoang, M. Hussain and D. Dochain, "Review and classification of recent observers applied in chemical process systems," *Computers and Chemical Engineering,* vol. 76, pp. 27-41, 2015.

[52] C. D. Massimo, M. J. Willis, G. Montague, M. T. Tham and . A. J. Morris, "Bioprocess model building using artificial neural networks," *Bioprocess Engineering* , vol. 7, pp. 77-82, 1991.

[53] F. Karbasi, H. Yunesi, M. Ardjmand, S. A. kordi, S. Yaghmaei and H. Qaderi, "Experimental investigation of poly-β-hydroxybutyrate production by Azohydromonas lata: Kinetics and artificial neural network modeling," *Chemical Engineering Communications,* pp. 1-47, 2014.

[54] X. Dai, W. Wang, Y. Ding and Z. Sun, ""“Assumed inherent sensor” inversion based ANN dynamic soft-sensing method and its application in erythromycin fermentation process," *Computers and Chemical Engineering,* vol. 30, p. 1203–1225, 2006.

[55] A. José de Assis and R. Maciel Filho, "Soft sensors development for on-line bioreactor state estimation," *Computers and Chemical Engineering ,* vol. 24, pp. 1099-1103, 2000.

[56] S. Ochoa, *Porcess Optimization Course,* Medellin, 2015.

[57] J. R. Banga, E. Balsa-Canto, C. G. Moles and A. A. Alonso, "Dynamic optimization of bioprocesses: Efficient and robust numerical strategies," *Journal of Biotechnology,* vol. 117, no. 4, p. 407–419, 2005.

[58] S. Khanna and A. K. Srivastava, "A Simple Structured Mathematical Model for Biopolymer (PHB) Production," *Biotechnology Progress,* vol. 21, no. 3, pp. 830-838, 2005.

[59] S. Ochoa, A. Yoo, J.-U. Repke, G. Wozny and D. R. Yang, "Modeling and Parameter Identification of the Simultaneous Saccharification-Fermentation Process for Ethanol Production," *Biotechnology Progress,* vol. 23, no. 16, p. 1454–1462, 2007.

[60] J. A. López , V. Bucalá and M. A. Villar, "Application of Dynamic Optimization Techniques for Poly(β-hydroxybutyrate) Production in a Fed-Batch Bioreactor.," *Ind. Eng. Chem. Res.,* vol. 49, p. 1762–1769, 2010.

[61] J. M. Naranjo Vasco , "Design and analysis of the polyhydroxybutyrate (PHB) production from agroindustrial wastes in Colombia," *Tesis Dcotorado: Universidad Nacional,* pp. 6-243, 2014.

[62] R. J. Van Wegen, Y. Ling and . A. P. J. Middelberg, "Industrial production of polyhydroxyalkanoates using escherichia coli: an economic analysis," *Trans IChemE,* vol. 76, pp. 1-10, 1998.

[63] J.-i. Choi and Y. L. Sang , "Process analysis and economic evaluation for Poly(3-hydroxybutyrate) production by fermentation," *Bioprocess Engineering ,* vol. 17 , p. 335±342, 1997.

[64] A. Villegas, J. P. Arias, D. Aragón, M. Arias and S. Ochoa, "Determination of the optimal operation conditions to maximize the biomass peruviana using multi-objective optimization," in *XXVII Congreso Interamericano y Colombiano de Ingeniería Química*, Cartagena-Colombia, 2014.

[65] O. Nida Sheibat , G. Févotte, D. Peycelon, . E. Jean-Bernard and . S. Jean-Marc, "Control of polymer molecular weight using near infrared spectroscopy," *AIChE Journal,* vol. 50, no. 3, p. 654–664, 2004.

[66] S. Kumar and D. Ramkrishna, "On the solution of population balance equations by discretization--i. a fixed pivot technique," *Chemical Engineering Science,* vol. 51, no. 8 , pp. 1311-1332, 1996.

[67] V. Saliakas, C. Chatzidoukas, A. Krallis, D. Meimaroglou and C. Kiparissides,

"Dynamic Optimization of Molecular Weight Distribution Using Orthogonal Collocation on Finite Elements and Fixed Pivot Methods: An Experimental and Theoretical Investigation," *Macromolecular Reaction Engineer,* vol. 1, p. 119–136, 2007.

[68] G. Penloglou, "Personal Communication," 2015.

[69] H. Alvares, "Course of Modelling of Dynamic System," *Universidad Nacional,* 2015.

[70] H. Hernández G and J. Aguirre C, "Molecular weight distribution estimation in batch polyesterification using a model-based soft sensor," *DYNA,* vol. 72, no. 147, pp. 65-73, 2005.

[71] M. Schlegel, K. Stockmann, T. Binder and W. Marquardt, "Dynamic optimization using adaptive control vector parameterization," *Computers and Chemical Engineering,* vol. 29, p. 1731–1751, 2005.